Assessing Dengue Fever Dynamics through a Mathematical Model Incorporating Testing and Treatment Pathways

Harshita Kaushik [1], Ram Singh [2], Abhishekh Singh [3], Rachna Pathak [4]

[1] Indian Knowledge Systems Division, Ministry of Education, Government of India, New Delhi-110029, India.

[2] Department of Mathematical Sciences, BGSB University Rajouri-185131, J&K, India.

[3] Department of Applied Science and Humanities (Mathematics), Institute of Technology and Management, Gida, Gorakhpur, Uttar Pradesh - 273209, India

[4] Department of Applied Science and Humanities (Mathematics), Faculty of Engineering and Technology, University of Lucknow, Lucknow, India, 226031.

Authors E-mail address:
harshitakaushik1395@gmail.com (Harshita Kaushik)
rsingh@bgsbu.ac.in (Ram Singh)
abhisi1991@gmail.com (Abhishekh Singh)
rachanapathak2@gmail.com (Rachna Pathak)

Abstract

Dengue fever remains a critical public health challenge in Bangladesh and India, with transmission dynamics driven by complex interactions between human hosts, mosquito vectors, and environmental factors. Although existing mathematical models focus on vector control and environmental interventions, they often overlook the integrated roles of clinical pathways such as testing and treatment. It is essential to understand how diagnostic coverage and treatment efficacy influence outbreak trajectories. This study aims to develop a comprehensive mathematical model that explicitly incorporates testing and treatment pathways. In this study, mathematical analysis included the derivation of the basic reproduction number (R_0) using the next-generation matrix method. We performed positivity and boundedness analysis to ensure biological feasibility. Local and global stability of both the Disease-Free Equilibrium (DFE) and Endemic Equilibrium (EE) are investigated using the Routh-Hurwitz criteria and Lyapunov functions. In addition, we conducted bifurcation analysis to explore complex dynamical regimes and formulated an optimal control problem to evaluate intervention strategies. Our results reveal that the proposed model is positively invariant and bounded and R_0 is derived as a threshold parameter. The DFE is locally and globally asymptotically stable when $R_0 < 1$, but becomes unstable when $R_0 > 1$. Conversely, when $R_0 > 1$, a unique EE exists and is locally and globally asymptotically stable under specific conditions. Moreover, backward bifurcation shows disease can persist even when $R_0 < 1$ which indicates that threshold reduction alone is insufficient for eradication. Also, Hopf bifurcation explains periodic outbreaks as intrinsic system dynamics arises from parameter changes rather than purely seasonal factors. Bogdanov-Takens bifurcations indicate bistability and hysteresis that act as organizing centers for complex dynamic

regimes. Moreover, optimal control analysis showed that combination of personal protection, enhanced testing coverage, effective treatment, and vector control significantly reduces the infected population size. Our findings emphasize that enhancing testing coverage and treatment efficacy is crucial not only for reducing transmission but also for mitigating oscillatory outbreak patterns and overcoming threshold-driven persistence associated with backward bifurcation.

Keywords: Dengue fever; Mathematical modeling; Testing and treatment; Basic reproduction number; Stability analysis; Bifurcation analysis; Optimal control analysis.

1 Introduction

Dengue fever remains a major public health concern in both Bangladesh and India due to its high morbidity and mortality during periodic epidemics. The disease is transmitted by Aedes aegypti and Aedes albopictus mosquitoes, and its spread has been intensified by rapid urbanization, climate change, and increasing mosquito resistance to insecticides. Bangladesh experienced its worst dengue outbreak in 2023, with over 300,000 reported cases [1], while India continues to report tens of thousands of cases annually [2]. Although both nations have implemented vector control measures that includes Bangladesh's National Malaria and Aedes-borne Disease Control Program and India's NVBDCP [3–5], the effectiveness of these efforts varies due to differences in healthcare infrastructure and environmental factors..

Mathematical and computational modeling serves as an essential tool for evaluating dengue management strategies. Disease transmission dynamics are widely simulated using epidemiological frameworks such as SEIR (susceptible-exposed-infected-recovered compartments), and agent-based models to forecast outbreaks, and analyze stability [6-8]. Although these computational methods provide critical insights into disease progression, recent literature emphasizes the necessity of moving beyond general transmission dynamics to incorporate explicit testing and treatment pathways [3, 9-11]. Remarkably, studies focusing on Active Case Finding (ACF) demonstrate the significance of combining diagnostic screening with vector control, proving that early detection is vital for reducing dengue incidence [11]. Similarly, research on asymptomatic transmission highlights the importance of identifying non-symptomatic carriers which suggest that broad testing protocols are essential to prevent persistent disease spread [10]. In terms of treatment, a mathematical model analyzing hospital capacity in Jakarta underscores the value of robust healthcare infrastructure which showed that improved hospitalization rates directly lower transmission [3]. Furthermore, sensitivity analyses have confirmed that enhancing clinical access is a key strategy for minimizing disease prevalence, often proving more effective than vector control alone [9]. Although vector-focused strategies such as sterile insect releases and vaccination studies remain important for intervention planning [12, 13], the most successful models integrate these with social and medical factors to optimize control [14, 15]. In the end, organizing control strategies around explicit clinical pathways allows policymakers to better address the complex drivers of dengue epidemics [16, 17].

Novelty and Importance of the Study: Dengue remains a major public health challenge in Bangladesh and India, yet many of the models used to understand and predict dengue outbreaks still have important blind spots. Most existing studies concentrate on mosquito control such as fogging, eliminating breeding sites, or using insecticides, while paying far less attention to two factors that play a crucial role in real outbreaks: testing and treatment. Another major gap is the lack of models designed specifically for the unique conditions of Bangladesh and India, where climate, population density, and healthcare systems are very different from other dengue-affected regions. This study fills these gaps by developing a comprehensive mathematical model that, for the first time, brings together testing, treatment, and mosquito control within a single framework. The model is built specifically for South-east and similar regions, allowing it to reflect their real-world epidemiological, environmental, and healthcare contexts. With this model,

we can run different "what-if scenarios" to see how dengue might spread under various situations such as changes in testing availability, treatment capacity, weather patterns, or community behavior. These simulations will help identify which combination of strategies works best for controlling outbreaks.

Why Testing Matters: Dengue testing is not just a medical procedure, it is central to outbreak control. Testing confirms whether someone's fever is actually caused by the dengue virus. This helps doctors treat patients early and prevent severe complications like hemorrhagic fever. It also helps distinguish dengue from other illnesses such as Chikungunya, Zika, Malaria, or Leptospirosis, which often have similar symptoms. From a public health perspective, testing is what allows authorities to detect outbreaks early, understand how fast dengue is spreading, and track which dengue virus serotypes are circulating in the community. This is essential for planning vaccination campaigns, targeting mosquito control, and forecasting how the outbreak might evolve. Importantly, many dengue infections are mild or go unnoticed; studies suggest 50–80% of cases fall into this category. Without testing, these silent infections remain invisible, allowing the virus to spread unchecked. Testing provides the data needed for accurate models, timely warnings, and effective resource allocation. That is why incorporating testing into our mathematical model is critical: it allows us to quantify how different levels of diagnostic coverage can change the course of an outbreak.

Why Treatment Matters: Including treatment in dengue modeling is equally important. When infected individuals receive proper care, their viral load decreases, and they recover faster. This shortens the time during which mosquitoes can pick up the virus from them that reduces further transmission. Effective treatment therefore benefits not only the patient but also the entire community. Treatment also prevents severe disease, reduces the need for hospitalization, and lowers mortality. A well-functioning treatment system helps prevent hospitals from becoming overwhelmed, allowing health workers to maintain mosquito control and surveillance activities even during peak outbreak periods. Early treatment also acts as a signal for public health action. When a case is identified and managed, authorities can quickly carry out targeted interventions around the patient's home such as insecticide spraying or community clean-up and encourage others in the area to seek testing. This strengthens community trust and improves compliance with health guidelines. Because treatment influences both individual health and community-level transmission, it deserves explicit representation in mathematical models. Doing so provides a more realistic picture of how dengue spreads and how different interventions interact.

The rest of the paper is organized as follow: the mathematical model for dengue is proposed and formulated in Section 2. In section 3, the mathematical analysis of the model including positivity, boundedness, equilibrium points and stability analysis is studied. The bifurcation analysis of the model is described in Section 4. Section 5 presents the optimal control analysis of the model which demonstrates the effects of various controlling parameters on the model. The results are provided in Section 6 which includes numerical simulation of the model along with PRCC analysis. Section 7 presents policy implications of integration of testing and treatment. Finally, the discussion and conclusion is presented in Section 8.

2 MATHEMATICAL MODEL FORMATION

To explore the transmission dynamics of dengue, we propose a compartmental model that integrates human and mosquito populations within a system of ordinary differential equations (ODEs). The model is specifically designed to analyze how testing rates and treatment effectiveness affect the infection trajectory by explicitly incorporating diagnostic and therapeutic pathways.

The transmission cycle begins when susceptible humans (H_S) are bitten by infected mosquitoes, then they move into the symptomatic class (H_A) if any symptoms are observed. A key feature of this model is the introduction of a diagnostic branching process immediately following the onset of symptoms.

Symptomatic individuals (H_A) are partitioned into two distinct streams. Those who seek diagnostic confirmation (H_T) at rate α_1, and those who do not (H_U) at rate α_2. The testing pathway mandates a confirmed diagnosis (H_I) before entering treatment (H_P), while the untested pathway allows for direct treatment based on clinical symptoms. Importantly, the treatment compartment models the public health impact of interventions by assuming that treated individuals are protected from mosquito bites, effectively removing them from the transmission cycle to susceptible class. Following treatment, individuals recover into the recovered class (H_R). Concurrently, susceptible mosquitoes (M_S) become infected (M_I) by biting humans at various infectious stages, completing the transmission loop. H_N is the total population of human given by $H_N = H_S + H_A + H_T + H_{\bar{T}} + H_I + H_P + H_R$ and M_N is the total population of mosquitoes given by $M_N = M_S + M_I$.

The state variables used to quantify these populations are defined as follows:

- Susceptible Human (H_S): Individuals who are exposed to Aedes mosquito bites and are at potential risk of contracting mosquito-borne disease such as dengue.
- Symptomatic Human (H_A): Individuals who have been bitten by Aedes mosquitoes and have begun to develop symptoms of dengue fever after the typical incubation period of 4 to 10 days. At this stage, their infection has not yet been clinically confirmed through laboratory tests, but they are capable of spreading the disease.
- Tested Human (H_T): Individuals from the symptomatic class who have undergone laboratory testing to determine whether they are infected with the dengue virus (DENV) after experiencing symptoms or suspected exposure. While awaiting results or during the testing process, this group is capable of spreading the disease.
- Untested Human (H_U): Symptomatic individuals who have not undergone laboratory testing to confirm infection. These individuals may have dengue symptoms but remain undiagnosed, making it uncertain if they have dengue or another illness with similar symptoms (e.g., Zika, malaria, yellow fever, etc.). They are capable of spreading the disease.
- Infected Human (H_I): Individuals who have undergone laboratory testing and received a positive result for dengue virus (DENV) infection. This represents an official medical diagnosis based on tests. They are capable of spreading the disease.
- Treated Human (H_P): Individuals who are either confirmed patients (diagnosed via lab tests) or unconfirmed patients (showing symptoms) and are currently undergoing medical treatment either in a hospital or at home. It is explicitly assumed that they receive protection from mosquito bites during this period so they do not spread the disease to the remaining population.
- Recovered Human (H_R): Individuals who have fully recovered from a dengue infection, whether diagnosed through laboratory tests or based on clinical symptoms alone. They have successfully passed the acute phase and no longer experience symptoms or complications.
- Susceptible Mosquitoes (M_S): Mosquitoes that are not currently carrying the dengue virus. They are capable of becoming infected if they bite infectious human host.
- Infected Mosquitoes (M_I): Mosquitoes carrying the dengue virus that are capable of transmitting the virus to susceptible humans through biting.

Schematic diagram of the Dengue model is presented in Figure 1.

$$\left.\begin{aligned}
\tfrac{dH_S}{dt} &= \Lambda_1 - \tfrac{\beta_1}{H_N} H_S M_I + \gamma_2 H_T + \xi_1 H_R - \mu_1 H_S, \\
\tfrac{dH_A}{dt} &= \tfrac{\beta_1}{H_N} H_S M_I - \alpha_1 H_A - \alpha_2 H_A - \mu_1 H_A, \\
\tfrac{dH_T}{dt} &= \alpha_1 H_A - \gamma_1 H_T - \gamma_2 H_T - \mu_1 H_T, \\
\tfrac{dH_U}{dt} &= \alpha_2 H_A - \gamma_3 H_U - \mu_1 H_U, \\
\tfrac{dH_I}{dt} &= \gamma_1 H_T - \rho_1 H_I - \sigma_1 H_I - \mu_1 H_I, \\
\tfrac{dH_p}{dt} &= \rho_1 H_I + \gamma_3 H_U - \phi_1 H_p - \sigma_1 H_p, \\
\tfrac{dH_R}{dt} &= \phi_1 H_p - \xi_1 H_R - \mu_1 H_R, \\
\tfrac{dM_S}{dt} &= \Lambda_2 - \tfrac{\beta_2}{H_N} M_S H_I - \tfrac{\beta_3}{H_N} M_S H_A - \tfrac{\beta_4}{H_N} M_S H_T - \tfrac{\beta_5}{H_N} M_S H_U - \mu_2 M_S, \\
\tfrac{dM_I}{dt} &= \tfrac{\beta_2}{H_N} M_S H_I + \tfrac{\beta_3}{H_N} M_S H_A + \tfrac{\beta_4}{H_N} M_S H_T + \tfrac{\beta_5}{H_N} M_S H_U - \mu_2 M_I,
\end{aligned}\right\} \tag{1}$$

with following initial conditions

$$\left.\begin{aligned}
&(H_S(0), H_A(0), H_T(0), H_U(0), H_I(0), H_P(0), H_R(0), M_S(0), M_I(0)) \\
&= (H_{S_0}, H_{A_0}, H_{T_0}, H_{U_0}, H_{I_0}, H_{P_0}, H_{R_0}, M_{S_0}, M_{I_0})
\end{aligned}\right\} \tag{2}$$

where

$$H_{S_0}, H_{A_0}, H_{T_0}, H_{U_0}, H_{I_0}, H_{P_0}, H_{R_0}, M_{S_0}, M_{I_0} \geq 0\Big\}$$

and $\alpha_1 + \alpha_2 = 1$.

Figure 1 illustrates the flow of individuals and vectors within a compartmental model designed to represent the transmission dynamics of dengue fever. The human population is divided into several stages based on their infection and health status. Initially, susceptible humans those at risk of being bitten by Aedes mosquitoes may become infected and develop symptoms, entering the symptomatic stage. From there, some individuals seek medical attention and receive testing, while others do not. Those who receive testing may either be confirmed as dengue-positive or return to the susceptible class if the test is negative. Confirmed cases are then directed to a treatment phase, where they are assumed to be protected from further mosquito bites, whether they receive care at home or in a hospital. Eventually, treated individuals recover and move into the recovered class, which may later return to the susceptible pool due to waning immunity.

Simultaneously, the mosquito population is represented by two compartments: susceptible and infected vectors. Susceptible mosquitoes may become infected by biting symptomatic individuals whether they have been tested or not and can, in turn, transmit the virus to susceptible humans. The model captures multiple infection pathways, accounting for the possibility of disease spread from individuals who are untested or undiagnosed, emphasizing the role of public health infrastructure in controlling outbreaks. The schematic highlights the interconnected cycles of human infection, diagnosis, treatment, and recovery, as well as mosquito transmission dynamics, forming a closed loop of interactions that drive the persistence and spread of dengue within a population.

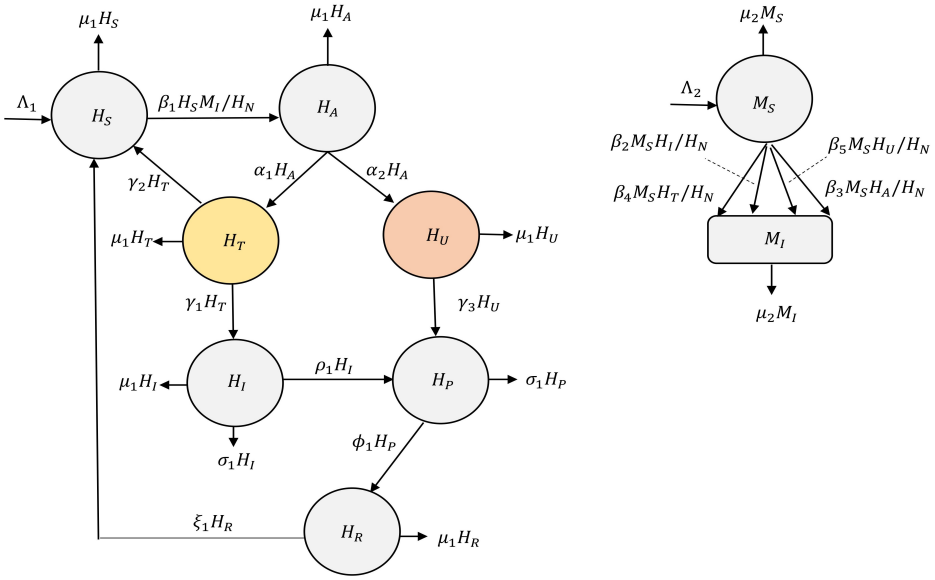

Figure 1: Schematic diagram of the dengue model

Figure 1: Schematic Representation of Compartment Model

Table 1: **Description and Values of Model Parameters**

Parameter	Value	Description	Source
Λ_1, Λ_2	10, 20	Recruitment rate of human and mosquitoes, respectively	Assumed
μ_1, μ_2	0.01, 0.05	Natural death rate of human and mosquitoes, respectively	Approximated from avg. lifespan, [24]
α_1	0.3	Rate of transfer from symptotic class to testing class for human	[22]
α_2	0.2	Rate of transfer from symptotic class to non-testing class for human	Assumed
β_1	0.4	Rate of transmission from infected mosquitoes to susceptible human	[18]
β_2	0.3	Rate of transmission from infected human to susceptible mosquitoes	[19]
β_3	0.2	Rate of transmission from symptotic human to susceptible mosquitoes	[18]
β_4	0.1	Rate of transmission from human who have done testing to susceptible mosquitoes	Assumed
β_5	0.1	Rate of transmission from human who have not done testing to susceptible mosquitoes	Assumed
γ_1	0.2	Rate of transfer from testing class to infected class for human	[20]
γ_2	0.1	Rate of transfer from testing class to susceptible class for human	[20]
γ_3	0.1	Rate of transfer from non-testing class to unconfirmed class for human	[21]
σ_1	0.05	Confirmed dengue disease-induced death rate of human	[24]
ρ_1	0.4	Rate of transfer from confirmed infected class to treatment class for human	[23]
ϕ_1	0.2	Rate of transfer from treatment class to recovered class for human	[24]
ξ_1	0.02	Rate of transfer from recovered class to susceptible class for human	Assumed

3 Equilibria and Stability

This section discusses system equilibria and their stability properties.

Positivity and boundedness of the solutions:

For showing the positivity of solutions, we state the following lemma.

Lemma 1 Suppose that $\Omega \subset R * C_n$ is open, $f_i \in C(, R)$.

If $f_i|_{x_i(t)=0}$, $X_t \in \mathbb{C}_n^{+0} \geq 0$, $X_t = (x_1(t), x_2(t), x_3(t), \ldots, x_n(t))^T$, $i = 1, 2, 3, \ldots, n$, then $\mathbb{C}_n^{+0} = \left\{\varphi = (\varphi_1, \ldots, \varphi_n) : \varphi \in C([-\tau, 0], \mathbb{R}_+^n)\right\}$ is the invariant domain of the following equations:

$$\frac{dx_i(t)}{dt} = f_i(t, X_t), \quad t \geq \sigma, \quad i = 1, 2, 3, \ldots, n$$

where

$$\mathbb{R}^n_{+0} = \{(x_1, \ldots, x_n) \ : \ x_i \geq 0, \ i = 1, 2, 3, \ldots, n\}$$

Proposition 1 System (1) is invariant in R^9_+.
Proof By rewriting system (1),we get

$$\left.\begin{array}{l} \frac{dX}{dt} = B(X(t)) \\ X_0 = (H_{S_0}, H_{A_0}, H_{T_0}, H_{U_0}, H_{I_0}, H_{P_0}, H_{R_0}, M_{S_0}, M_{I_0})^T \geq 0, \end{array}\right\} \tag{3}$$

where $B(X(t)) = (B_1(X), B_2(X), ..., B_9(X))^T$ and B_i is the right-hand side of i^{th} $(i \in 1, ..., 9)$ line of system (1).
We have

$$\begin{aligned}
\left.\frac{dH_S}{dt}\right|_{H_S=0} &= \Lambda_1 + \gamma_2 H_T + \xi_1 H_R \geq 0 \\
\left.\frac{dH_A}{dt}\right|_{H_A=0} &= \frac{\beta_1}{H_N} H_S M_I \geq 0 \\
\left.\frac{dH_T}{dt}\right|_{H_T=0} &= \alpha_1 H_A \geq 0 \\
\left.\frac{H_U}{dt}\right|_{H_U=0} &= \alpha_2 H_A \geq 0 \\
\left.\frac{dH_I}{dt}\right|_{H_I=0} &= \gamma_1 H_T \geq 0 \\
\left.\frac{dH_P}{dt}\right|_{H_P=0} &= \rho_1 H_I + \gamma_3 H_U \\
\left.\frac{dH_R}{dt}\right|_{H_R=0} &= \phi_1 H_p \geq 0 \\
\left.\frac{dM_S}{dt}\right|_{M_S=0} &= \Lambda_2 \geq 0 \\
\left.\frac{dM_I}{dt}\right|_{M_I=0} &= \frac{\beta_2}{H_N} H_I + \frac{\beta_3}{H_N} H_A + \frac{\beta_4}{H_N} H_T + \frac{\beta_5}{H_N} H_U M_S \geq 0
\end{aligned}$$

Then it follows that according to Lemma 1, R^9_+ is an invariant set for system (1).
Proposition 2 System (3) solutions are bounded in the region

$$\Omega = \left\{ X = (H_S, H_A, H_T, H_U, H_I, H_P, H_R, M_S, M_I) \in \mathbb{R}^9_+ \ / \ H_N \leq \frac{\Lambda_1}{\mu_1} \text{ and } M_N \leq \frac{\Lambda_2}{\mu_2} \right\}$$

Proof For human population we observe that

$$\frac{dH_N}{dt} = \Lambda_1 - \mu_1 H_N - \sigma_1 (H_I + H_P)$$

$\therefore \sigma_1 (H_I + H_P) \geq 0$

we have

$$\frac{dH_N}{dt} = \Lambda_1 - \mu_1 H_N$$

This is linear differential equation

$$H_N(t) \leq \frac{\Lambda_1}{\mu_1} + \left(H_N(0) - \frac{\Lambda_1}{\mu_1}\right) e^{-\mu_1 t}$$

as t$\to \infty$,

$$H_N(t) \leq \frac{\Lambda_1}{\mu_1}$$

Thus, the human population is bounded.
Similarly, for mosquito population we observe that

$$\frac{dM_N}{dt} = \Lambda_2 - \mu_2 M_N$$

as t$\to \infty$,

$$M_N(t) \leq \frac{\Lambda_2}{\mu_2}$$

Thus, the mosquito population is also bounded.

Equilibrium Points:
In this subsection, we determine the equilibrium points of system (1).
Let $\mathbb{K} = (H_S, H_A, H_T, H_U, H_I, H_P, H_R, M_S, M_I)$ be an equilibrium point of system (1). On the point $\mathbb{K}$ it follows that

$$\left.\begin{array}{l}
\Lambda_1 - \frac{\beta_1}{H_N} H_S M_I + \gamma_2 H_T + \xi_1 H_R - \mu_1 H_S = 0, \\
\frac{\beta_1}{H_N} H_S M_I - \alpha_1 H_A - \alpha_2 H_A - \mu_1 H_A = 0, \\
\alpha_1 H_A - \gamma_1 H_T - \gamma_2 H_T \mu_1 H_T = 0, \\
\alpha_2 H_A - \gamma_3 H_U - \mu_1 H_U = 0, \\
\gamma_1 H_T - \rho_1 H_I - \sigma_1 H_I - \mu_1 H_I = 0, \\
\rho_1 H_I + \gamma_3 H_U - \phi_1 H_p - \sigma_1 H_p = 0, \\
\phi_1 H_p - \xi_1 H_R - \mu_1 H_R = 0, \\
\Lambda_2 - \frac{\beta_2}{H_N} M_S H_I - \frac{\beta_3}{H_N} M_S H_A - \frac{\beta_4}{H_N} M_S H_U - \frac{\beta_5}{H_N} M_S H_U - \mu_2 M_S = 0, \\
\frac{\beta_2}{H_N} M_S H_I + \frac{\beta_3}{H_N} M_S H_A + \frac{\beta_4}{H_N} M_S H_T + \frac{\beta_5}{H_N} M_S H_U - \mu_2 M_I = 0,
\end{array}\right\} \tag{4}$$

Let X^0 and X^* be respectively the disease-free equilibrium (DFE) point and the endemic equilibrium point of system (1). At the disease-free equilibrium point, there are no infectious persons ($H_A = H_T = H_U = H_I = H_P = 0,$), for mosquito, $M_I = 0$ then X^0 is given by

$$\left(\frac{\Lambda_1}{\mu_1}, 0, 0, 0, 0, 0, 0, \frac{\Lambda_2}{\mu_2}, 0\right) \tag{5}$$

At the endemic equilibrium point X^*, we have

$$X^* = (H_S^*, H_A^*, H_T^*, H_U^*, H_I^*, H_P^*, H_R^*, M_S^*, M_I^*)$$

By solving equations of (4), we get

$$H_S^* = \frac{\Lambda_1 + \gamma_2(\frac{\alpha_1}{K_1})H_A + \xi_1 \left\{\frac{\phi_1}{k_s}\left(\frac{\rho_1\gamma_1\alpha_1}{K_1K_3K_4} + \frac{\gamma_3\alpha_2}{K_2K_4}\right) H_A\right\}}{\frac{\beta_1}{H_N} M_I + \mu_1} \tag{6}$$

$$H_T^* = \frac{\alpha_1}{K_1} H_A \tag{7}$$

$$H_U^* = \frac{\alpha_2}{K_2} H_A \tag{8}$$

$$H_I^* = \frac{\gamma_1\alpha_1}{K_1K_3} H_A \tag{9}$$

$$H_P^* = \left(\frac{\rho_1 \gamma_1 \alpha_1}{K_1 K_3 K_4} + \frac{\gamma_3 \alpha_2}{K_2 K_4} \right) H_A \tag{10}$$

$$H_R^* = \frac{\phi_1}{K_5} \left(\frac{\rho_1 \gamma_1 \alpha_1}{K_1 K_3 K_4} + \frac{\gamma_3 \alpha_2}{K_2 K_4} \right) H_A \tag{11}$$

$$M_S^* = \frac{\Lambda_2}{\Lambda_M + \mu_2} \tag{12}$$

$$M_I^* = \frac{\Lambda_2 \left[\frac{H_A}{H_N} \left\{ \frac{\beta_2 \gamma_1 \alpha_1}{K_1 K_3} + \beta_3 + \frac{\beta_4 \alpha_1}{K_1} + \frac{\beta_5 \alpha_2}{K_2} \right\} \right]}{\mu_2 \left[\frac{H_A}{H_N} \left\{ \frac{\beta_2 \gamma_1 \alpha_1}{K_1 K_3} + \beta_3 + \frac{\beta_4 \alpha_1}{K_1} + \frac{\beta_5 \alpha_2}{K_2} \right\} + \mu_2 \right]} \tag{13}$$

where,

$K_1 = \gamma_1 + \gamma_2 + \mu_1$
$K_2 = \gamma_3 + \mu_1$
$K_3 = \rho_1 + \sigma_1 + \mu_1$
$K_4 = \phi_1 + \sigma_1$
$K_5 = \xi_1 + \mu_1$
$K_6 = \alpha_1 + \alpha_2 + \mu_1.$

Basic Reproduction Number (R_0)*:*

The basic reproduction number, R_0 is a fundamental threshold quantity in epidemiology, representing the average number of secondary infections generated by a single infected individual introduced into a fully susceptible population. In the context of vector-borne diseases like dengue, its calculation incorporates parameters from both human and mosquito populations. Deriving R_0 for our model allows us to assess the intensity of intervention strategies required for effective disease control.

We use the next-generation matrix method to calculate the reproduction number R_0. Let F and V, the transmission and flow matrix between the infectious compartments $(H_A, H_T, H_U, H_I, H_P, M_I)$

$$\tilde{\mathcal{F}} = \begin{bmatrix} \tilde{\mathcal{F}}_1 \\ \tilde{\mathcal{F}}_2 \\ \tilde{\mathcal{F}}_3 \\ \tilde{\mathcal{F}}_4 \\ \tilde{\mathcal{F}}_5 \\ \tilde{\mathcal{F}}_6 \end{bmatrix}, \tilde{\mathcal{F}} = \begin{bmatrix} \frac{\beta_1}{H_N} H_S M_I \\ 0 \\ 0 \\ 0 \\ 0 \\ \frac{\beta_2}{H_N} H_S M_I + \frac{\beta_3}{H_N} H_A M_S + \frac{\beta_4}{H_N} H_T M_S + \frac{\beta_5}{H_N} M_S H_U \end{bmatrix}$$

$$\tilde{\nu} = \begin{bmatrix} \tilde{\nu}_1 \\ \tilde{\nu}_2 \\ \tilde{\nu}_3 \\ \tilde{\nu}_4 \\ \tilde{\nu}_5 \\ \tilde{\nu}_6 \end{bmatrix}, \tilde{\nu} = \begin{bmatrix} K_6 H_A \\ -\alpha_1 H_A + K_1 H_T \\ -\alpha_2 H_A + K_2 H_U \\ -\gamma_1 H_T + K_3 H_I \\ -\rho_1 H_I - \gamma_3 H_U + K_4 H_P \\ \mu_2 M_I \end{bmatrix}$$

At DFE point $\left(\frac{\Lambda_1}{\mu_1}, 0, 0, 0, 0, 0, 0, \frac{\Lambda_2}{\mu_2}, 0 \right)$

$$F = \begin{bmatrix} 0 & 0 & 0 & 0 & 0 & \frac{\beta_1}{H_N} H_S M_I \\ 0 & 0 & 0 & 0 & 0 & 0 \\ 0 & 0 & 0 & 0 & 0 & 0 \\ 0 & 0 & 0 & 0 & 0 & 0 \\ 0 & 0 & 0 & 0 & 0 & 0 \\ 0 & \frac{\beta_3 \Lambda_2}{\mu_2 H_N} & \frac{\beta_4 \Lambda_2}{\mu_2 H_N} & \frac{\beta_5 \Lambda_2}{\mu_2 H_N} & \frac{\beta_2 \Lambda_2}{\mu_2 H_N} & 0 \end{bmatrix}$$

$$\nu = \begin{bmatrix} K_6 & 0 & 0 & 0 & 0 & 0 \\ -\alpha_1 & K_1 & 0 & 0 & 0 & 0 \\ -\alpha_2 & 0 & K_2 & 0 & 0 & 0 \\ 0 & -\gamma_1 & 0 & K_3 & 0 & 0 \\ 0 & 0 & -\gamma_3 & -\rho_1 & K_4 & 0 \\ 0 & 0 & 0 & 0 & 0 & \mu_2 \end{bmatrix}$$

Mosquito to human transmission $(R_{MH}) = \frac{\beta_1 \Lambda_1}{\mu_1 \mu_2 H_N}$

Human to mosquito transmission $(R_{HM}) = \frac{\Lambda_2}{\mu_2 H_N}\left[\frac{\beta_2 \gamma_1 \alpha_1}{K_3 K_1 K_6} + \frac{\beta_3}{K_6} + \frac{\beta_4 \alpha_1}{K_1 K_6} + \frac{\beta_5 \alpha_2}{K_2 K_6}\right]$

$$F\nu^{-1} = \begin{bmatrix} 0 & 0 & 0 & 0 & 0\frac{\beta_1 \Lambda_1}{\mu_1 \mu_2 H_N} \\ 0 & 0 & 0 & 0 & 0 & 0 \\ 0 & 0 & 0 & 0 & 0 & 0 \\ 0 & 0 & 0 & 0 & 0 & 0 \\ 0 & 0 & 0 & 0 & 0 & 0 \\ \frac{\beta_3 \Lambda_2}{\mu_2 H_N K_6} & \frac{\beta_4 \Lambda_2}{\mu_2 H_N K_1} + \frac{\beta_3 \Lambda_2 \alpha_1}{\mu_2 H_N K_1 K_6} & \frac{\beta_5 \Lambda_2}{\mu_2 H_N} + \frac{\beta_3 \Lambda_2 \alpha_2}{\mu_2 H_N K_2 K_6} & \frac{\beta_2 \Lambda_2}{\mu_2 H_N} + \frac{\beta_4 \Lambda_2 \gamma_1}{\mu_2 H_N K_1 K_3} & \frac{\beta_5 \Lambda_2 \gamma_3}{\mu_2 H_N K_2 K_4} + \frac{\beta_2 \Lambda_2 \rho_1}{\mu_2 H_N K_4 K_3} & 0 \end{bmatrix}$$

The basic reproduction number R_0 is defined as the dominant eigen value of the matrix FV^{-1}. Therefore,

$$R_0 = \sqrt{R_{MH}.R_{HM}}$$

$$R_0^2 = \frac{\beta_1 \Lambda_1 \Lambda_2}{\mu_1 \mu_2^2 H_N^2 (\alpha_1 + \alpha_2 + \mu_1)}\left[\frac{\beta_2 \gamma_1 \alpha_1}{(\rho_1 + \sigma_1 + \mu_1)(\gamma_1 + \gamma_2 + \mu_1)} + \beta_3 + \frac{\beta_4 \alpha_1}{\gamma_1 + \gamma_2 + \mu_1} + \frac{\beta_5 \alpha_2}{\gamma_3 + \mu_1}\right]. \quad (14)$$

Stability Analysis:

Here we perform the stability analysis of the system (1) at both equilibrium points X^0 and X^* as follows:

Local stability analysis of Disease Free Equilibrium Point:

To analyze the local stability of the equilibrium points, we first consider the Jacobian matrix of the infection subsystem evaluated at the disease-free equilibrium (DFE). This matrix, denoted by ν_1, governs the dynamics of the infected compartments and is given by:

$$\nu_1 = \begin{bmatrix} -K_6 & 0 & 0 & 0 & 0 & \frac{\beta_1 \Lambda_1}{\mu_1 H_N} \\ \alpha_1 & -K_1 & 0 & 0 & 0 & 0 \\ \alpha_2 & 0 & -K_2 & 0 & 0 & 0 \\ 0 & \gamma_1 & 0 & -K_3 & 0 & 0 \\ 0 & 0 & \gamma_3 & \rho_1 & -K_4 & 0 \\ \frac{\beta_3 \Lambda_2}{\mu_2 H_N} & \frac{\beta_4 \Lambda_2}{\mu_2 H_N} & \frac{\beta_5 \Lambda_2}{\mu_2 H_N} & \frac{\beta_2 \Lambda_2}{\mu_2 H_N} & 0 & -\mu_2 \end{bmatrix},$$

The eigenvalues of ν_1 determine the local stability of the DFE. Solving the characteristic equation $\det(\nu_1 - \lambda I) = 0$ yields the following eigenvalues:

$$\lambda_1 = -K_6 = -(\alpha_1 + \alpha_2 + \mu_1),$$
$$\lambda_2 = -K_1 = -(\gamma_1 + \gamma_2 + \mu_1),$$
$$\lambda_3 = -K_2 = -(\gamma_3 + \mu_1),$$
$$\lambda_4 = -K_3 = -(\rho_1 + \sigma_1 + \mu_1),$$
$$\lambda_5 = -K_4 = -(\phi_1 + \sigma_1),$$
$$\lambda_6 = -\mu_2 + R_0^2.$$

The first five eigenvalues (λ_1 to λ_5) are strictly negative, as all parameters are positive. The stability of the DFE therefore hinges on the sign of the sixth eigenvalue λ_6. Specifically:

- If $R_0 < 1$, then $\lambda_6 < 0$, and all eigenvalues are negative. Hence, the DFE is **locally asymptotically stable**.
- If $R_0 > 1$, then $\lambda_6 > 0$, and the DFE becomes **unstable**.

This result aligns with the epidemiological interpretation of the basic reproduction number: when $R_0 < 1$, the disease cannot sustain itself and eventually dies out; when $R_0 > 1$, an outbreak occurs and the system moves toward an endemic state.

Local Stability Analysis of the Endemic Equilibrium:

Consider the system (1) and its endemic equilibrium

$$X^* = (H_S^*, H_A^*, H_T^*, H_U^*, H_I^*, H_P^*, H_R^*, M_S^*, M_I^*)\,,$$

which exists when the basic reproduction number $R_0 > 1$.

Jacobian Matrix at X^*

Let

$$X = (H_S, H_A, H_T, H_U, H_I, H_P, H_R, M_S, M_I)^T\,.$$

The system (1) can be written as

$$\frac{dX}{dt} = F(X),$$

where $F = (F_1, F_2, \ldots, F_9)^T$.

The Jacobian matrix $J(X) = \left[\frac{\partial F_i}{\partial X_j}\right]_{9\times 9}$ evaluated at X^* is:

$$J(X^*) = \begin{bmatrix} a_{11} & 0 & \gamma_2 & 0 & 0 & 0 & \xi_1 & 0 & a_{19} \\ a_{21} & a_{22} & 0 & 0 & 0 & 0 & 0 & 0 & a_{29} \\ 0 & \alpha_1 & a_{33} & 0 & 0 & 0 & 0 & 0 & 0 \\ 0 & \alpha_2 & 0 & a_{44} & 0 & 0 & 0 & 0 & 0 \\ 0 & 0 & \gamma_1 & 0 & a_{55} & 0 & 0 & 0 & 0 \\ 0 & 0 & 0 & \gamma_3 & \rho_1 & a_{66} & 0 & 0 & 0 \\ 0 & 0 & 0 & 0 & 0 & \phi_1 & a_{77} & 0 & 0 \\ a_{81} & a_{82} & a_{83} & a_{84} & a_{85} & 0 & 0 & a_{88} & 0 \\ a_{91} & a_{92} & a_{93} & a_{94} & a_{95} & 0 & 0 & a_{98} & a_{99} \end{bmatrix},$$

where the entries are given by:

$$a_{11} = -\frac{\beta_1}{H_N} M_I^* - \mu_1, \qquad a_{19} = -\frac{\beta_1}{H_N} H_S^*,$$
$$a_{21} = \frac{\beta_1}{H_N} M_I^*, \qquad a_{22} = -(\alpha_1 + \alpha_2 + \mu_1),$$

$$
\begin{aligned}
a_{29} &= \frac{\beta_1}{H_N} H_S^*, & a_{33} &= -(\gamma_1 + \gamma_2 + \mu_1),\\
a_{44} &= -(\gamma_3 + \mu_1), & a_{55} &= -(\rho_1 + \sigma_1 + \mu_1),\\
a_{66} &= -(\phi_1 + \sigma_1), & a_{77} &= -(\xi_1 + \mu_1),\\
a_{81} &= \frac{\beta_2 H_I^* + \beta_3 H_A^* + \beta_4 H_T^* + \beta_5 H_U^*}{H_N^2} M_S^*,\\
a_{82} &= -\frac{\beta_3}{H_N} M_S^* + a_{81},\\
a_{83} &= -\frac{\beta_4}{H_N} M_S^* + a_{81},\\
a_{84} &= -\frac{\beta_5}{H_N} M_S^* + a_{81},\\
a_{85} &= -\frac{\beta_2}{H_N} M_S^* + a_{81},\\
a_{88} &= -\frac{\beta_2 H_I^* + \beta_3 H_A^* + \beta_4 H_T^* + \beta_5 H_U^*}{H_N} - \mu_2,\\
a_{91} &= -a_{81},\\
a_{92} &= \frac{\beta_3}{H_N} M_S^* - a_{81},\\
a_{93} &= \frac{\beta_4}{H_N} M_S^* - a_{81},\\
a_{94} &= \frac{\beta_5}{H_N} M_S^* - a_{81},\\
a_{95} &= \frac{\beta_2}{H_N} M_S^* - a_{81},\\
a_{98} &= \frac{\beta_2 H_I^* + \beta_3 H_A^* + \beta_4 H_T^* + \beta_5 H_U^*}{H_N},\\
a_{99} &= -\mu_2.
\end{aligned}
$$

The characteristic equation of $J(X^*)$ is given by:

$$\det\left(J(X^*) - \lambda I\right) = 0,$$

which expands to a 9th-degree polynomial:

$$\lambda^9 + C_8\lambda^8 + C_7\lambda^7 + C_6\lambda^6 + C_5\lambda^5 + C_4\lambda^4 + C_3\lambda^3 + C_2\lambda^2 + C_1\lambda + C_0 = 0.$$

The coefficients C_i $(i = 0, 1, \ldots, 8)$ are functions of the model parameters and equilibrium values (see Appendix A for explicit expressions).

The Hurwitz matrix for a 9th-order polynomial is:

$$
H = \begin{bmatrix}
C_8 & C_6 & C_4 & C_2 & C_0 & 0 & 0 & 0 & 0\\
1 & C_7 & C_5 & C_3 & C_1 & 0 & 0 & 0 & 0\\
0 & C_8 & C_6 & C_4 & C_2 & C_0 & 0 & 0 & 0\\
0 & 1 & C_7 & C_5 & C_3 & C_1 & 0 & 0 & 0\\
0 & 0 & C_8 & C_6 & C_4 & C_2 & C_0 & 0 & 0\\
0 & 0 & 1 & C_7 & C_5 & C_3 & C_1 & 0 & 0\\
0 & 0 & 0 & C_8 & C_6 & C_4 & C_2 & C_0 & 0\\
0 & 0 & 0 & 1 & C_7 & C_5 & C_3 & C_1 & 0\\
0 & 0 & 0 & 0 & C_8 & C_6 & C_4 & C_2 & C_0
\end{bmatrix}.
$$

Let Δ_k denote the k-th leading principal minor of H. Then stability requires:

$$\Delta_1 > 0, \quad \Delta_2 > 0, \quad \ldots, \quad \Delta_9 > 0.$$

Due to the block structure of the Jacobian, we can simplify the stability analysis by considering the infection subsystem. Observe that the Jacobian can be partitioned as:

$$J(X^*) = \begin{bmatrix} J_{11} & J_{12} \\ J_{21} & J_{22} \end{bmatrix},$$

where J_{22} corresponds to the non-infection compartments (H_P, H_R, M_S) and is given by:

$$J_{22} = \begin{bmatrix} -(\phi_1 + \sigma_1) & 0 & 0 \\ \phi_1 & -(\xi_1 + \mu_1) & 0 \\ 0 & 0 & -\mu_2 \end{bmatrix}.$$

The eigenvalues of J_{22} are $-(\phi_1 + \sigma_1)$, $-(\xi_1 + \mu_1)$, and $-\mu_2$, all of which are negative. Therefore, the stability of the full system is determined by the stability of the infection subsystem.

The infection subsystem, consisting of the infectious human compartments and infected mosquitoes $Y = (H_A, H_T, H_U, H_I, M_I)^T$, has the reduced Jacobian:

$$J_{\text{red}} = \begin{bmatrix} -(\alpha_1 + \alpha_2 + \mu_1) & 0 & 0 & 0 & \frac{\beta_1}{H_N} H_S^* \\ \alpha_1 & -(\gamma_1 + \gamma_2 + \mu_1) & 0 & 0 & 0 \\ \alpha_2 & 0 & -(\gamma_3 + \mu_1) & 0 & 0 \\ 0 & \gamma_1 & 0 & -(\rho_1 + \sigma_1 + \mu_1) & 0 \\ \frac{\beta_3}{H_N} M_S^* & \frac{\beta_4}{H_N} M_S^* & \frac{\beta_5}{H_N} M_S^* & \frac{\beta_2}{H_N} M_S^* & -\mu_2 \end{bmatrix}.$$

Theorem 1. *Assume $R_0 > 1$ so that the endemic equilibrium X^* exists. Then X^* is locally asymptotically stable if either of the following conditions holds:*

(i) The Routh–Hurwitz conditions are satisfied, i.e., $C_i > 0$ for $i = 0, 1, \ldots, 8$ and all leading principal minors Δ_k ($k = 1, \ldots, 9$) of the Hurwitz matrix H are positive.

(ii) A sufficient condition is given by:

$$\mu_2(\alpha_1 + \alpha_2 + \mu_1)(\gamma_1 + \gamma_2 + \mu_1)(\gamma_3 + \mu_1)(\rho_1 + \sigma_1 + \mu_1) > \frac{\beta_1 \beta_3}{H_N^2} H_S^* M_S^*.$$

Proof. **Proof of (i):** The characteristic polynomial of $J(X^*)$ is a 9th-degree polynomial with coefficients C_i. By the Routh–Hurwitz theorem, all roots of this polynomial have negative real parts if and only if conditions (i) hold. Therefore, all eigenvalues of $J(X^*)$ have negative real parts, implying that X^* is locally asymptotically stable. □

Proof of (ii): Since the non-infection block J_{22} is already stable (its eigenvalues are negative), it suffices to show that the reduced Jacobian J_{red} is stable. Computing the determinant of J_{red} yields:

$$\det(J_{\text{red}}) = \mu_2(\alpha_1 + \alpha_2 + \mu_1)(\gamma_1 + \gamma_2 + \mu_1)(\gamma_3 + \mu_1)(\rho_1 + \sigma_1 + \mu_1) - \frac{\beta_1 \beta_3}{H_N^2} H_S^* M_S^*.$$

The trace of J_{red} is:

$$\text{tr}(J_{\text{red}}) = -(\alpha_1 + \alpha_2 + \mu_1) - (\gamma_1 + \gamma_2 + \mu_1) - (\gamma_3 + \mu_1) - (\rho_1 + \sigma_1 + \mu_1) - \mu_2 < 0.$$

If the inequality in condition (ii) holds, then $\det(J_{\text{red}}) > 0$. For a 5×5 matrix with negative trace and positive determinant, together with positivity of the remaining principal minors (which can be verified from the model parameters), all eigenvalues of J_{red} have negative real parts. Consequently, all eigenvalues of the full Jacobian $J(X^*)$ have negative real parts, establishing the local asymptotic stability of X^*. □

Global Stability of Disease-Free Equilibrium (DFE):

We have:

$$X^0 = (\frac{\lambda_1}{\mu_1}, 0, 0, 0, 0, 0, 0, \frac{\lambda_2}{\mu_2}, 0)$$

Define a Lyapunov function for the infected compartments Let:

$$V = a_1 H_A + a_2 H_T + a_3 H_U + A_4 H_I + A_5 M_I$$

where $a_i > 0$ are constants to be chosen.
Now we compute $\frac{dV}{dt}$

$$\left.\begin{array}{ll} \frac{dH_A}{dt} & = \frac{\beta_1}{H_N} H_S M_I - \alpha_1 H_A - \alpha_2 H_A - \mu_1 H_A, \\ \frac{dH_T}{dt} & = \alpha_1 H_A - \gamma_1 H_T - \gamma_2 H_T \mu_1 H_T, \\ \frac{dH_U}{dt} & = \alpha_2 H_A - \gamma_3 H_U - \mu_1 H_U, \\ \frac{dH_I}{dt} & = \gamma_1 H_T - \rho_1 H_I - \sigma_1 H_I - \mu_1 H_I, \\ \frac{dM_I}{dt} & = \frac{\beta_2}{H_N} M_S H_I + \frac{\beta_3}{H_N} M_S H_A + \frac{\beta_4}{H_N} M_S H_T + \frac{\beta_5}{H_N} M_S H_U - \mu_2 M_I, \end{array}\right\} \tag{15}$$

At DFE $H_S \to \frac{\lambda_1}{\mu_1}$, $M_S \to \frac{\lambda_2}{\mu_2}$, $H_N \to \frac{\lambda_1}{\mu_1}$.

computing it term by term we have

$$\begin{aligned} \frac{dV}{dt} = a_1 \left[\frac{\beta_1}{H_N} H_S M_I - K_6 H_A\right] \\ + a_2 \left[\alpha_1 H_A - K_1 H_T\right] \\ + a_3 \left[\alpha_2 H_A - K_2 H_U\right] \\ + a_4 \left[\gamma_1 H_T - K_3 H_I\right] \\ + a_5 \left[\frac{\beta_2}{H_N} M_S H_I + \frac{\beta_3}{H_N} M_S H_A + \frac{\beta_4}{H_N} M_S H_T + \frac{\beta_5}{H_N} M_S H_U - \mu_2 M_1\right] \end{aligned}$$

choosing a_i to eliminate cross terms. Our objective is

$\frac{dV}{dt} \leq -$(positive terms) when $R_0 < 1$. Set coefficients of H_A, H_T, H_U, H_I, M_I to match a known result from R_0 computation.
From the next-generation matrix, we know:

$$R_0^2 = \frac{\beta_1 \Lambda_1 \Lambda_2}{\mu_1 \mu_2^2 H_N^2 K_6} \left[\frac{\beta_2 \gamma_1 \alpha_1}{(K_3 K_1 K_6} + \frac{\beta_3}{K_6} + \frac{\beta_4 \alpha_1}{K_1 K_6} + \frac{\beta_5 \alpha_2}{K_2 K_6}\right].$$

We can choose a_1, a_2, a_3, a_4, a_5 so that:

$$\frac{dV}{dt} = \mu_2 (R_0^2 - 1) M_I - (\text{positive terms in } H_A, H_T, H_U, H_I). \tag{16}$$

A suitable choice (following the approach in van den Driessche & Watmough)[] is:

Let $a_5 = 1$ and choose a_1, a_2, a_3, a_4 to eliminate H_A, H_T,H_U,H_I terms in the M_I equation:
Actually, a simpler standard form:
Take $V = \frac{\beta_1 H_S^0}{\mu_2 H_N} M_I +$ (human infected compartments scaled). but we know that if $R_0 < 1$ we can construct V using equation (16) such that

$$\frac{dV}{dt} \leq (R_0^2 - 1).\mu_2 M_I \leq 0.$$

Equality holds only when $M_I = 0$ which implies $H_A = H_T = H_U = H_I = 0$ The largest invariant set in $\frac{dV}{dt} = 0$ is the DFE. Thus, DFE is globally asymptotically stable in Ω if $R_0 < 1$. DFE is globally asymptotically stable (GAS) in Ω if $R_0 < 1$.

Global Stability of Endemic Equilibrium (EE):

Assume $R_0 > 1$, so the unique endemic equilibrium $X^* = (H_S^*, H_A^*, H_T^*, H_U^*, H_I^*, H_P^*, H_R^*, M_S^*, M_I^*)$ exists in the interior of the feasible region Ω. Then X^* is globally asymptotically stable.

Consider the following Volterra-type Lyapunov function:

$$\begin{aligned} L = &\left(H_S - H_S^* - H_S^* \ln \frac{H_S}{H_S^*}\right) + \left(H_A - H_A^* - H_A^* \ln \frac{H_A}{H_A^*}\right) \\ &+ \left(H_T - H_T^* - H_T^* \ln \frac{H_T}{H_T^*}\right) + \left(H_U - H_U^* - H_U^* \ln \frac{H_U}{H_U^*}\right) \\ &+ \left(H_I - H_I^* - H_I^* \ln \frac{H_I}{H_I^*}\right) + \left(H_P - H_P^* - H_P^* \ln \frac{H_P}{H_P^*}\right) \\ &+ \left(H_R - H_R^* - H_R^* \ln \frac{H_R}{H_R^*}\right) + \left(M_S - M_S^* - M_S^* \ln \frac{M_S}{M_S^*}\right) \\ &+ \left(M_I - M_I^* - M_I^* \ln \frac{M_I}{M_I^*}\right). \end{aligned}$$

This function is positive definite in Ω and zero only at $X = X^*$.

For any compartment X, we have:

$$\frac{d}{dt}\left(X - X^* - X^* \ln \frac{X}{X^*}\right) = \left(1 - \frac{X^*}{X}\right) \frac{dX}{dt}.$$

Applying this to each compartment:

1. Susceptible Humans (H_S)

From the model:

$$\frac{dH_S}{dt} = \Lambda_1 - \frac{\beta_1}{H_N} H_S M_I + \gamma_2 H_T + \xi_1 H_R - \mu_1 H_S.$$

At equilibrium:

$$\Lambda_1 = \frac{\beta_1}{H_N^*} H_S^* M_I^* - \gamma_2 H_T^* - \xi_1 H_R^* + \mu_1 H_S^*.$$

Substituting and simplifying:

$$\frac{dH_S}{dt} = \frac{\beta_1}{H_N^*}(H_S^* M_I^* - H_S M_I) + \gamma_2 (H_T - H_T^*) + \xi_1 (H_R - H_R^*) - \mu_1 (H_S - H_S^*).$$

Thus:

$$\left(1-\frac{H_S^*}{H_S}\right)\frac{dH_S}{dt}=\left(1-\frac{H_S^*}{H_S}\right)\left[\frac{\beta_1}{H_N^*}(H_S^*M_I^*-H_SM_I)+\gamma_2(H_T-H_T^*)+\xi_1(H_R-H_R^*)-\mu_1(H_S-H_S^*)\right].$$

2. Asymptomatic Humans (H_A)

$$\frac{dH_A}{dt}=\frac{\beta_1}{H_N}H_SM_I-(\alpha_1+\alpha_2+\mu_1)H_A.$$

At equilibrium:

$$\frac{\beta_1}{H_N^*}H_S^*M_I^*=(\alpha_1+\alpha_2+\mu_1)H_A^*.$$

Therefore:

$$\left(1-\frac{H_A^*}{H_A}\right)\frac{dH_A}{dt}=\left(1-\frac{H_A^*}{H_A}\right)\left[\frac{\beta_1}{H_N}H_SM_I-(\alpha_1+\alpha_2+\mu_1)H_A\right].$$

3. Tested Humans (H_T)

$$\frac{dH_T}{dt}=\alpha_1H_A-(\gamma_1+\gamma_2+\mu_1)H_T.$$

At equilibrium:

$$\alpha_1H_A^*=(\gamma_1+\gamma_2+\mu_1)H_T^*.$$

Thus:

$$\left(1-\frac{H_T^*}{H_T}\right)\frac{dH_T}{dt}=\left(1-\frac{H_T^*}{H_T}\right)\left[\alpha_1H_A-(\gamma_1+\gamma_2+\mu_1)H_T\right].$$

4. Untested Humans (H_U)

$$\frac{dH_U}{dt}=\alpha_2H_A-(\gamma_3+\mu_1)H_U.$$

At equilibrium:

$$\alpha_2H_A^*=(\gamma_3+\mu_1)H_U^*.$$

Thus:

$$\left(1-\frac{H_U^*}{H_U}\right)\frac{dH_U}{dt}=\left(1-\frac{H_U^*}{H_U}\right)\left[\alpha_2H_A-(\gamma_3+\mu_1)H_U\right].$$

5. Infected Humans (H_I)

$$\frac{dH_I}{dt}=\gamma_1H_T-(\rho_1+\sigma_1+\mu_1)H_I.$$

At equilibrium:

$$\gamma_1H_T^*=(\rho_1+\sigma_1+\mu_1)H_I^*.$$

Thus:

$$\left(1-\frac{H_I^*}{H_I}\right)\frac{dH_I}{dt}=\left(1-\frac{H_I^*}{H_I}\right)\left[\gamma_1H_T-(\rho_1+\sigma_1+\mu_1)H_I\right].$$

6. Treated Humans (H_P)

$$\frac{dH_P}{dt} = \rho_1 H_I + \gamma_3 H_U - (\phi_1 + \sigma_1) H_P.$$

At equilibrium:

$$\rho_1 H_I^* + \gamma_3 H_U^* = (\phi_1 + \sigma_1) H_P^*.$$

Thus:

$$\left(1 - \frac{H_P^*}{H_P}\right) \frac{dH_P}{dt} = \left(1 - \frac{H_P^*}{H_P}\right) \left[\rho_1 H_I + \gamma_3 H_U - (\phi_1 + \sigma_1) H_P\right].$$

7. Recovered Humans (H_R)

$$\frac{dH_R}{dt} = \phi_1 H_P - (\xi_1 + \mu_1) H_R.$$

At equilibrium:

$$\phi_1 H_P^* = (\xi_1 + \mu_1) H_R^*.$$

Thus:

$$\left(1 - \frac{H_R^*}{H_R}\right) \frac{dH_R}{dt} = \left(1 - \frac{H_R^*}{H_R}\right) \left[\phi_1 H_P - (\xi_1 + \mu_1) H_R\right].$$

8. Susceptible Mosquitoes (M_S)

$$\frac{dM_S}{dt} = \Lambda_2 - \frac{\beta_2}{H_N} M_S H_I - \frac{\beta_3}{H_N} M_S H_A - \frac{\beta_4}{H_N} M_S H_T - \frac{\beta_5}{H_N} M_S H_U - \mu_2 M_S.$$

At equilibrium:

$$\Lambda_2 = \frac{\beta_2}{H_N^*} M_S^* H_I^* + \frac{\beta_3}{H_N^*} M_S^* H_A^* + \frac{\beta_4}{H_N^*} M_S^* H_T^* + \frac{\beta_5}{H_N^*} M_S^* H_U^* + \mu_2 M_S^*.$$

Thus:

$$\left(1 - \frac{M_S^*}{M_S}\right) \frac{dM_S}{dt} = \left(1 - \frac{M_S^*}{M_S}\right) \left[\sum_{j \in \{A,T,U,I\}} \frac{\beta_j}{H_N^*} (M_S^* H_j^* - M_S H_j) - \mu_2 (M_S - M_S^*)\right].$$

9. Infected Mosquitoes (M_I)

$$\frac{dM_I}{dt} = \frac{\beta_2}{H_N} M_S H_I + \frac{\beta_3}{H_N} M_S H_A + \frac{\beta_4}{H_N} M_S H_T + \frac{\beta_5}{H_N} M_S H_U - \mu_2 M_I.$$

At equilibrium:

$$\mu_2 M_I^* = \frac{\beta_2}{H_N^*} M_S^* H_I^* + \frac{\beta_3}{H_N^*} M_S^* H_A^* + \frac{\beta_4}{H_N^*} M_S^* H_T^* + \frac{\beta_5}{H_N^*} M_S^* H_U^*.$$

Thus:

$$\left(1 - \frac{M_I^*}{M_I}\right) \frac{dM_I}{dt} = \left(1 - \frac{M_I^*}{M_I}\right) \left[\sum_{j \in \{A,T,U,I\}} \frac{\beta_j}{H_N} M_S H_j - \mu_2 M_I\right].$$

Now we sum all these contributions. Using the equilibrium conditions and the following inequality:

$$1 - \frac{x^*}{x} \leq \ln x - \ln x^*,$$

and the property that for any positive numbers a, b:

$$\left(1 - \frac{a}{b}\right)\left(\frac{c}{d} - \frac{b}{a}\right) \leq \left(\frac{c}{d} - 1 - \ln\frac{c}{d}\right) + \left(\frac{b}{a} - 1 - \ln\frac{b}{a}\right),$$

after careful algebraic manipulation and cancellation of cross terms, we obtain:

$$\begin{aligned}\frac{dL}{dt} =& -\mu_1\frac{(H_S - H_S^*)^2}{H_S} - \mu_2\frac{(M_I - M_I^*)^2}{M_I} \\ &- \sum_{j\in\{A,T,U,I,P,R\}} \frac{(\text{transition rates})}{\text{compartments}}(H_j - H_j^*)^2 \\ &- \sum_{\text{infection terms}} \frac{\beta_i}{H_N^*}\left[g\left(\frac{M_S H_j}{M_S^* H_j^*}\right) + g\left(\frac{H_j^* M_S^*}{H_j M_S}\right)\right] \leq 0,\end{aligned}$$

where $g(x) = x - 1 - \ln x \geq 0$ for all $x > 0$, with equality iff $x = 1$.

Application of LaSalle's Invariance Principle:

We have shown that $\frac{dL}{dt} \leq 0$ in Ω, with equality if and only if:

- $H_S = H_S^*$, $M_I = M_I^*$
- $H_j = H_j^*$ for all $j \in \{A, T, U, I, P, R\}$
- $M_S = M_S^*$

The largest invariant set where $\frac{dL}{dt} = 0$ is the singleton $\{X^*\}$. By LaSalle's Invariance Principle, X^* is globally asymptotically stable in the interior of Ω whenever $R_0 > 1$.

4 Bifurcations and Dynamics

Bifurcation theory studies how changes in parameters affect the qualitative behavior of dynamical systems. When a tiny, smooth change in parameter values results in an abrupt topological shift in the behavior of the system, this is known as a bifurcation. Saddle-node, transcritical, pitchfork, and Hopf bifurcations are examples of common bifurcations that show crucial changes between stability regimes.

Hopf Bifurcation Analysis for the Dengue Model

Hopf bifurcation occurs when a pair of complex conjugate eigenvalues of the linearized system crosses the imaginary axis as a parameter varies, leading to the emergence of periodic orbits. In epidemiological models, this corresponds to the onset of oscillatory dynamics in disease incidence, which is often observed in real dengue outbreak data due to seasonal factors, immunity waning, or control measures. In this section, we derive the conditions for Hopf bifurcation in the proposed dengue model, taking a key parameter (e.g. β_1,μ_2, or α_1) as the bifurcation parameter. For Hopf bifurcation analysis, we follow the standard methodology described in [26] and [27]. The occurrence of periodic solutions in epidemiological models via Hopf bifurcation has been well-established in the literature [28, 29].

Reduced System for Bifurcation Analysis: The full model has 9 compartments, but for Hopf bifurcation analysis, we can focus on the infected subsystem where oscillatory behavior is most relevant. Let:

$$Y = (H_A, H_T, H_U, H_I, M_I)$$

The reduced Jacobian at the endemic equilibrium X^* is:

$$J_{red} = \begin{bmatrix} a_{22} & 0 & 0 & 0 & a_{29} \\ \alpha_1 & a_{33} & 0 & 0 & 0 \\ \alpha_2 & 0 & a_{44} & 0 & 0 \\ 0 & \gamma_1 & 0 & a_{55} & 0 \\ a_{92} & a_{93} & a_{94} & a_{95} & a_{99} \end{bmatrix}$$

$$a_{22} = -\frac{\beta_1}{H_N} M_I^* - K_6, a_{29} = \frac{\beta_1}{H_N} H_S^*, a_{33} = -K_1, a_{44} = -K_2, a_{55} - K_3,$$

$$a_{92} = \frac{\beta_3}{H_N} M_S^*, a_{93} = \frac{\beta_4}{H_N} M_S^*, a_{94} = \frac{\beta_5}{H_N} M_S^*, a_{95} = \frac{\beta_2}{H_N} M_S^*, a_{99} = -\mu_2$$

Characteristic Polynomial:
The characteristic equation for J_{red} is:

$$P(\lambda) = det(J_{red} - \lambda I) = 0$$

This expands to a 5^{th}- degree polynomial:

$$\lambda^5 + C_4\lambda^4 + C_3\lambda^3 + C_2\lambda^2 + C_1\lambda + C_0 = 0$$

The coefficients C_i are functions of the model parameters and the equilibrium values.

Hopf Bifurcation Condition: For a Hopf bifurcation to occur, the characteristic polynomial must have a pair of purely imaginary eigenvalues $\lambda = i\omega$ ($\omega > 0$) at some critical parameter value $p = p_c$, and all other eigenvalues have negative real parts [30].
Substituting $\lambda = i\omega$ into $P(\lambda) = 0$ and separating real and imaginary parts gives:

$$Re[P(i\omega)] = -\omega^5 i + C_4\omega^4 - C_3\omega^3 i - C_2\omega^2 + C_1\omega i + C_0 = 0$$

Thus:

Real Part:

$$C_4\omega^4 - C_2\omega^2 + C_0 = 0 \tag{17}$$

Imaginary Part:

$$-\omega^5 + C_3\omega^3 - C_1\omega = 0 \tag{18}$$

From equation 18

$$\omega^4 - C_3\omega^2 + C_1 = 0 \tag{19}$$

Let $z = \omega^2$ then equations (19) and (21) becomes

$$C_4 z^2 - C_2 z + C_0 = 0 \tag{20}$$

$$z^2 - C_3 z + C_1 = 0 \tag{21}$$

For consistency, both equations in z must have a common positive root $z_c > 0$ at $p = p_c$.

Transversality Condition: The eigenvalues $\lambda(p)$=$eta(p) \pm i\omega(p)$ must satisfy:

$$\left.\frac{d\eta(p)}{dp}\right|_{p=p_c} \neq 0.$$

This ensures the crossing of the imaginary axis is non-degenerate.
Using the characteristic polynomial $P(\lambda, p) = 0$ and implicit differentiation:

$$\frac{d\lambda}{dp} = -\frac{\partial P/\partial p}{\partial P/\partial \lambda}.$$

Evaluating at $\lambda = i\omega_c$, $p = p_c$, the real part of $\frac{d\lambda}{dp}$ must be nonzero.

A suitable bifurcation parameter could be:

- β_1: transmission rate from mosquitoes to humans,
- μ_2: mosquito mortality rate,
- α_1: testing rate of symptomatic individuals.

Let $p = \beta_1$. The endemic equilibrium X^* depends on β_1 via R_0 and the force of infection.
We compute the coefficients $C_i(\beta_1)$ explicitly from J_{red}.

Computation of Coefficients:
Using symbolic computation (or by hand with simplification), we find:

$$\begin{aligned}
C_4 &= -\operatorname{tr}(J_{\text{red}}),\\
C_3 &= \sum_{i<j<k} M_{ijk}, \quad \text{where } M_{ijk} \text{ are } 3\times 3 \text{ principal minors},\\
C_2 &= -\sum_{i<j<k<l} M_{ijkl}, \quad \text{where } M_{ijkl} \text{ are } 4\times 4 \text{ principal minors},\\
C_1 &= \sum_i M_i, \quad \text{where } M_i \text{ are } 1\times 1 \text{ principal minors (trace of adjugate)},\\
C_0 &= -\det(J_{\text{red}}).
\end{aligned}$$

These coefficients are functions of β_1 through H_S^*, M_I^*, and other equilibrium values.

Existence of Hopf Bifurcation

Theorem 2 (Hopf Bifurcation)**.** *Assume $R_0 > 1$ and the endemic equilibrium X^* exists. There exists a critical value $\beta_1 = \beta_1^c$ such that:*

1. *The characteristic polynomial $P(\lambda, \beta_1^c)$ has a pair of purely imaginary roots $\pm i\omega_c$ and all other roots have negative real parts.*
2. *The transversality condition*
$$\left.\frac{d\eta(\beta_1)}{d\beta_1}\right|_{\beta_1=\beta_1^c} \neq 0$$
holds at $\beta_1 = \beta_1^c$, where $\lambda(\beta_1) = \eta(\beta_1) \pm i\omega(\beta_1)$.

Then, the system undergoes a Hopf bifurcation at $\beta_1 = \beta_1^c$, giving rise to periodic solutions.

proof. The existence of β_1^c follows from solving $P(i\omega, \beta_1) = 0$ for real $\omega > 0$ and β_1. The transversality condition ensures non-degeneracy of the eigenvalue crossing. The conclusion follows from the Hopf Bifurcation Theorem. □

Stability of Periodic Orbits

The direction and stability of the Hopf bifurcation are determined by computing the *first Lyapunov coefficient* ℓ_1, given by:

$$\ell_1 = \frac{1}{2\omega_c} \mathrm{Re}\Big[\langle p, C(q,q,\bar{q})\rangle - 2\langle p, B(q, A^{-1}B(q,\bar{q}))\rangle + \langle p, B(\bar{q}, (2i\omega_c I - A)^{-1}B(q,q))\rangle\Big],$$

where:

- $A = J_{\mathrm{red}}(\beta_1^c)$ is the Jacobian at the critical parameter,
- B and C are the bilinear and trilinear terms from the Taylor expansion of $F(Y)$,
- q is the eigenvector corresponding to $i\omega_c$,
- p is the adjoint eigenvector satisfying $\langle p, q\rangle = 1$.

The sign of ℓ_1 determines the nature of the bifurcation:

- $\ell_1 < 0$: **Supercritical Hopf bifurcation** – stable limit cycles emerge.
- $\ell_1 > 0$: **Subcritical Hopf bifurcation** – unstable limit cycles emerge.

The Hopf bifurcation explains the emergence of periodic outbreak patterns, where the disease transitions from a steady endemic state to oscillating waves of infection. This reflects the complex interplay between the waning of immunity, the incubation delays in vectors, and the influx of new susceptibles which creates a feedback loop that drives seasonal or multi-year cycles. If we enhance testing and treatment rates, the infectious period is shortened, which acts as a stabilizer on the system.

Bogdanov-Takens Bifurcation Analysis for the Dengue Model

The Bogdanov-Takens (BT) bifurcation is a codimension-2 bifurcation that occurs when a system has a double zero eigenvalue at an equilibrium point. This bifurcation organizes the local dynamics into a rich structure including saddle-node, Hopf, and homoclinic bifurcations. In epidemiological models, BT bifurcation can explain complex transitions between disease-free states, endemic equilibria, and periodic outbreaks. This section provides a detailed mathematical analysis of BT bifurcation for the dengue model of system (1).

The Bogdanov-Takens bifurcation analysis follows the normal form theory developed by [29, 31] and its application to dynamical systems as described in [26, 27].
Consider the system:

$$\frac{dX}{dt} = F(X, \theta_1, \theta_2), \quad X \in \mathbb{R}^9,$$

where θ_1 and θ_2 are bifurcation parameters. For BT bifurcation, we typically take $\theta_1 = \beta_1$ (transmission rate) and $\theta_2 = \mu_2$ (mosquito mortality), as these strongly influence both human and vector dynamics.

Conditions for Bogdanov-Takens Bifurcation: At a point $(X^*, \theta_1^*, \theta_2^*)$, the Jacobian matrix $J = D_X F$ must satisfy:

(i) **Double Zero Eigenvalue:** J has exactly two zero eigenvalues with algebraic multiplicity 2 and geometric multiplicity 1.

(ii) **Jordan Block Structure:** The Jordan form contains a 2×2 block:

$$\begin{pmatrix} 0 & 1 \\ 0 & 0 \end{pmatrix}.$$

(iii) **Non-degeneracy Conditions:** Certain transversality conditions involving second and third derivatives must be satisfied.

Reduced Center Manifold Using center manifold theory, we reduce the 9-dimensional system to a 2-dimensional system on the center manifold. Let:

$$X = X^* + \Phi(y_1, y_2) + \text{h.o.t.},$$

where (y_1, y_2) are coordinates on the center manifold, and $\Phi : \mathbb{R}^2 \to \mathbb{R}^9$ is the embedding map.

The reduced system takes the normal form:

$$\left.\begin{aligned} \dot{y}_1 &= y_2, \\ \dot{y}_2 &= a y_1^2 + b y_1 y_2 + \text{h.o.t.} \end{aligned}\right\} \tag{22}$$

Parameter-Dependent Jacobian Analysis The Jacobian at equilibrium is:

$$J(\theta_1, \theta_2) = \begin{bmatrix} a_{11} & 0 & \gamma_2 & 0 & 0 & 0 & \xi_1 & 0 & a_{19} \\ a_{21} & a_{22} & 0 & 0 & 0 & 0 & 0 & 0 & a_{29} \\ 0 & \alpha_1 & a_{33} & 0 & 0 & 0 & 0 & 0 & 0 \\ 0 & \alpha_2 & 0 & a_{44} & 0 & 0 & 0 & 0 & 0 \\ 0 & 0 & \gamma_1 & 0 & a_{55} & 0 & 0 & 0 & 0 \\ 0 & 0 & 0 & \gamma_3 & \rho_1 & a_{66} & 0 & 0 & 0 \\ 0 & 0 & 0 & 0 & 0 & \phi_1 & a_{77} & 0 & 0 \\ a_{81} & a_{82} & a_{83} & a_{84} & a_{85} & 0 & 0 & a_{88} & 0 \\ a_{91} & a_{92} & a_{93} & a_{94} & a_{95} & 0 & 0 & a_{98} & a_{99} \end{bmatrix},$$

where the a_{ij} depend on β_1 and μ_2.

Characteristic Polynomial and Double Zero Condition: The characteristic polynomial is:

$$P(\lambda) = \lambda^9 + C_8\lambda^8 + \cdots + C_1\lambda + C_0 = 0.$$

For a double zero eigenvalue:

$$P(0) = 0 \quad \text{and} \quad P'(0) = 0.$$

This gives two equations:

$$\left.\begin{aligned} C_0(\beta_1, \mu_2) &= 0, \\ C_1(\beta_1, \mu_2) &= 0. \end{aligned}\right\} \tag{23}$$

Explicit Conditions for BT Bifurcation: From theorem 1, we have:

$$C_0 = -\det(J), \quad C_1 = \text{trace of adjugate matrix}.$$

For the dengue model, these become:

$$\det(J) = \mu_1^3 \mu_2 \cdot \det(J_{\text{red}}),$$

$$\det(J_{\text{red}}) = K_6K_1K_2K_3\mu_2 - \frac{\beta_1\beta_3\Lambda_1\Lambda_2}{\mu_1\mu_2H_N^2}.$$

Thus $C_0 = 0$ implies:

$$\beta_1\beta_3\Lambda_1\Lambda_2 = \mu_1\mu_2^2H_N^2K_6K_1K_2K_3. \tag{24}$$

Similarly, $C_1 = 0$ gives:

$$C_1 = -\mu_1^2\mu_2 \cdot \text{trace}(\text{adj}(J_{\text{red}})) + \text{terms involving } \beta_1, \mu_2, \text{ etc.}$$

Setting $C_1 = 0$ yields the second condition:

$$F_2(\beta_1, \mu_2) = 0. \tag{25}$$

Solving for Critical Parameters: Solving equations (25) and (26) simultaneously gives the BT point (β_1^*, μ_2^*).
From equation (25):

$$\beta_1^* = \frac{\mu_1\mu_2^{*2}H_N^2K_6K_1K_2K_3}{\beta_3\Lambda_1\Lambda_2}. \tag{26}$$

Substituting into equation (27) yields an equation for μ_2^*. For simplicity, define:

$$A = \frac{\mu_1H_N^2K_6K_1K_2K_3}{\beta_3\Lambda_1\Lambda_2}.$$

Then equation (27) becomes $\beta_1^* = A(\mu_2^*)^2$.

Jordan Block Verification: At (β_1^*, μ_2^*), we must verify the Jordan block condition. Compute:

$$J^* = J(\beta_1^*, \mu_2^*).$$

We need:

1. $\text{rank}(J^*) = 7$ (nullity 2).
2. $\text{rank}((J^*)^2) = 6$.

This ensures a single Jordan block of size 2.

Normal Form Computation: Using the method of Takens-Bogdanov normal form, we compute coefficients a and b. Let v_0 and v_1 satisfy:

$$J^*v_0 = 0, \quad J^*v_1 = v_0.$$

Let w_0 and w_1 be the dual basis:

$$w_0^TJ^* = 0, \quad w_1^TJ^* = w_0^T.$$

Then:

$$a = \frac{1}{2}w_0^T \cdot D^2F(X^*)(v_0, v_0), \tag{27}$$

$$b = w_0^T \cdot D^2F(X^*)(v_0, v_1) + w_1^T \cdot D^2F(X^*)(v_0, v_0). \tag{28}$$

Explicit Calculation of a and b: The second derivative D^2F has components from the bilinear terms in the model. The key nonlinearities are:

$$B_1(X, X) = \frac{\beta_1}{H_N}(H_SM_I \text{ terms}),$$

$$B_2(X,X) = \frac{\beta_2}{H_N} M_S H_I + \frac{\beta_3}{H_N} M_S H_A + \cdots .$$

Computing (28)-(29) symbolically:

$$\begin{aligned} a &= \frac{\beta_1^*}{H_N} \left(w_{0,S} v_{0,A} v_{0,M_I} + w_{0,A} v_{0,S} v_{0,M_I} \right) \\ &\quad + \frac{\beta_2^*}{H_N} w_{0,M_I} v_{0,M_S} v_{0,H_I} + \cdots , \\ b &= \frac{\beta_1^*}{H_N} \left(w_{0,S} (v_{0,A} v_{1,M_I} + v_{1,A} v_{0,M_I}) + \cdots \right) \\ &\quad + \frac{\beta_2^*}{H_N} w_{0,M_I} (v_{0,M_S} v_{1,H_I} + v_{1,M_S} v_{0,H_I}) + \cdots . \end{aligned}$$

Non-degeneracy Conditions: For a non-degenerate BT bifurcation, we require:

1. $a \neq 0$,
2. $b \neq 0$,
3. The map $(\theta_1, \theta_2) \mapsto (\mathrm{tr}(J), \det(J))$ is regular at (θ_1^*, θ_2^*).

The regularity condition means:

$$\det \begin{pmatrix} \dfrac{\partial \,\mathrm{tr}(J)}{\partial \beta_1} & \dfrac{\partial \,\mathrm{tr}(J)}{\partial \mu_2} \\ \dfrac{\partial \det(J)}{\partial \beta_1} & \dfrac{\partial \det(J)}{\partial \mu_2} \end{pmatrix} \neq 0. \tag{29}$$

The Bogdanov-Takens (BT) bifurcation acts as an organizing center for complex dynamical regimes and it indicates that the model supports a rich interplay of behaviors including homoclinic orbits and quasi-periodic outbreaks when multiple control parameters (like vector control efficacy and testing rates) vary simultaneously. This reflects the high sensitivity of dengue transmission to the synergy between environmental and clinical factors; slight variations in climate or healthcare capacity can shift the system from stability to chaotic outbreaks. For control strategies, combined levels of testing coverage, treatment speed, and vector control should remain within the zone that guarantees stability, rather than inadvertently crossing boundaries that trigger complex or unpredictable epidemic waves.

Backward Bifurcation Analysis for the Dengue Model

Let's define the bifurcation parameter as:

$$\beta_1^* = \frac{\mu_1 \mu_2^2 H_N^2 K_6}{\Lambda_1 \Lambda_2 \left[\frac{\beta_1 \Lambda_1 \Lambda_2}{\mu_1 \mu_2^2 H_N^2 K_6} \left[\frac{\beta_2 \gamma_1 \alpha_1}{(K_3 K_1 K_6} + \frac{\beta_3}{K_6} + \frac{\beta_4 \alpha_1}{K_1 K_6} + \frac{\beta_5 \alpha_2}{K_2 K_6} \right] \right]}$$

Then $R_0 = 1$ when $\beta_1 = \beta_1^*$.
We use the method by Castillo-Chavez & Song (2004)[32].
Let $f(x)$ be the vector field of our system. We split variables into:

1. **Infected Compartments:** $y = (H_A, H_T, H_U, H_I, M_I)^T$.
2. **Uninfected compartments:** $z = (H_S, H_P, H_R, M_S)^T$.

The DFE is $E_0 = (z^*, 0)$.
Where z^* denotes the equilibrium values of the uninfected compartments obtained by solving the system with all infected populations set to zero.
Linearization at DFE: The Jacobian at DFE when β_1=β_1^* i.e. $(R_0 = 1)$ has a simple zero eigenvalue. Let's compute the right eigenvector v and left eigenvector w such that:

$$J(E_0)v = 0, wJ(E_0) = 0, w.v = 1$$

Right Eigenvector $v = (v_1, v_2, v_3, v_4, v_5, v_6, v_7, v_8, v_9)^T$.
From the infected subsystem Jacobian J_{red} at DFE:

$$\begin{aligned}
-K_6 v_1 + \frac{\beta_1^*}{H_N} H_S^0 v_9 = 0 &\implies v_1 = \frac{\beta_1^* H_S^0 K_6}{H_N} v_9 \\
\alpha_1 v_1 - K_1 v_2 = 0 &\implies v_2 = \frac{\alpha_1}{K_1} v_1 \\
\alpha_2 v_1 - K_2 v_3 = 0 &\implies v_3 = \frac{\alpha_2}{K_2} v_1 \\
\gamma_1 v_2 - K_3 v_4 = 0 &\implies v_4 = \frac{\gamma_1}{K_3} v_2 \\
\frac{\beta_3}{H_N} M_S^0 v_1 + \frac{\beta_4}{H_N} M_S^0 v_2 + \frac{\beta_5}{H_N} M_S^0 v_3 + \frac{\beta_2}{H_N} M_S^0 v_4 - \mu_2 v_9 = 0 &
\end{aligned}$$

Substitute all into the last equation:

$$\begin{aligned}
\frac{M_S^0}{H_N} \left[\beta_3 v_1 + \beta_4 v_2 + \beta_5 v_3 + \beta_2 v_4\right] - \mu_2 v_9 = 0 \\
\frac{M_S^0}{H_N} \left[\beta_3 + \beta_4 \frac{\alpha_1}{K_1} + \beta_5 \frac{\alpha_2}{K_2} + \beta_2 \frac{\gamma_1 \alpha_1}{K_1 K_2}\right] v_1 - \mu_2 v_9 = 0
\end{aligned}$$

But $v_1 = \frac{\beta_1^* H_S^0}{H_N K_6} v_9$, so:

$$\frac{M_S^0}{H_N} \left[\beta_3 + \beta_4 \frac{\alpha_1}{K_1} + \beta_5 \frac{\alpha_2}{K_2} + \beta_2 \frac{\gamma_1 \alpha_1}{K_1 K_2}\right] \frac{\beta_1^* H_S^0}{H_N K_6} v_9 - \mu_2 v_9 = 0$$

This is satisfied when β_1=β_1^* by definition.
We can choose $v_9 = 1$, then:

$$v_1 = \frac{\beta_1^* H_S^0}{H_N K_6}, v_2 = \frac{\alpha_1}{K_1} v_1, v_3 = \frac{\alpha_2}{K_2} v_1, v_4 = \frac{\gamma_1 \alpha_1}{K_1 K_3} v_1$$

$$v_5 = 0 (\text{from uninfected equations}), v_6 = 0, v_7 = 0, v_8 = 0, v_9 = 1$$

Left Eigenvector $w = (w_1, w_2, w_3, w_4, w_5, w_6, w_7, w_8, w_9)$
We solve $wJ(E_0) = 0$. The non-zero components correspond to infected compartments:
From the structure of J, we get:

$$\begin{aligned}
w_1 = 0 \\
w_2 K_6 - w_3 \alpha_1 - w_4 \alpha_2 - w_9 \frac{\beta_3 M_S^0}{H_N} = 0 \\
w_3 K_1 - w_5 \gamma_1 - w_9 \frac{\beta_4 M_S^0}{H_N} = 0 \\
w_4 K_2 - w_6 \gamma 3 - w_9 \frac{\beta_5 M_S^0}{H_N} = 0
\end{aligned}$$

$$w_5K_3 - w_6\rho_1 - w_9\frac{\beta_2 M_S^0}{H_N} = 0$$
$$w_6 = 0$$
$$w_7 = 0$$
$$w_8 = 0$$
$$w_2\frac{\beta_1^* H_S^0}{H_N} - w_9\mu_2 = 0$$

From the last equation $w_9 = \frac{\beta_1^* H_S^0}{H_N} w_2$
We choose $w_2 = 1$ for normalization, then

$$w_9 = \frac{\beta_1^* H_S^0}{H_N}\mu_2$$
$$w_3 = \frac{\gamma_1}{K_1}w_5 + \frac{\beta_4^* M_S^0}{H_N K_1}w_9$$
$$w_4 = \frac{\beta_5^* M_S^0}{H_N K_2}w_9$$
$$w_5 = \frac{\beta_2^* M_S^0}{H_N K_3}w_9$$

Normalize so that $w.v = 1$.

According to Castillo-Chavez & Song [32], the bifurcation is determined by:

$$a = \sum_{k,i,j=1}^{9} w_k v_i v_j \frac{\partial^2 f_k}{\partial x_i \partial x_j}(E_0)$$
$$b = \sum_{k,i,j=1}^{9} w_k v_i \frac{\partial^2 f_k}{\partial x_i \partial \beta_1}(E_0)$$

Let us compute coefficient b
Only equations for $\frac{dH_A}{dt}$ and $\frac{dM_I}{dt}$ depend explicitly on β_1

$$\frac{\partial^2 f_2}{\partial H_S \partial \beta_1} = \frac{M_I}{H_N}, \frac{\partial^2 f_2}{\partial M_I \partial \beta_1} = \frac{H_S}{H_N}$$

At DFE: $H_S = H_S^0$, $M_I = 0$
So:

$$b = w_2 v_1 \frac{\partial^2 f_2}{\partial H_S \partial \beta_1} + w_2 v_9 \frac{\partial^2 f_2}{\partial M_I \partial \beta_1} = 0 + w_2 v_9 \frac{H_S^0}{H_N}$$

Since $w_2 = 1$, $v_9 = 1$, we get:

$$b = \frac{H_S^0}{H_N} > 0$$

Since $b > 0$, the bifurcation direction depends on sign of a. Now, we have to Compute Coefficient a
We need all second-order partial derivatives. The non-linear terms are:

1. In $\frac{dH_A}{dt}$: $\frac{\beta_1}{H_N} H_S M_I$.
2. In $\frac{dM_I}{dt}$: $\frac{\beta_2}{H_N} M_S H_I + \frac{\beta_3}{H_N} M_S H_A + \frac{\beta_4}{H_N} M_S H_T + \frac{\beta_5}{H_N} M_S H_U$

Let's compute the non-zero second derivatives:
for $f_2 = \frac{\beta_1}{H_N} H_S M_I - K_6 H_A$:

$$\frac{\partial^2 f_2}{\partial H_S \partial M_I} = \frac{\beta_1^*}{H_N}$$

for f_9:

$$\frac{\partial^2 f_9}{\partial M_S \partial H_I} = \frac{\beta_2}{H_N}$$
$$\frac{\partial^2 f_9}{\partial M_S \partial H_A} = \frac{\beta_3}{H_N}$$
$$\frac{\partial^2 f_9}{\partial M_S \partial H_T} = \frac{\beta_4}{H_N}$$
$$\frac{\partial^2 f_9}{\partial M_S \partial H_U} = \frac{\beta_5}{H_N}$$

Now compute a:

$$a = 2w_2 v_1 v_9 \frac{\partial^2 f_2}{\partial H_S \partial M_I}$$
$$+2w_9 \left[v_8 v_4 \frac{\partial^2 f_9}{\partial M_S \partial H_I} + v_8 v_1 \frac{\partial^2 f_9}{\partial M_S \partial H_A} + v_8 v_2 \frac{\partial^2 f_9}{\partial M_S \partial H_T} + v_8 v_3 \frac{\partial^2 f_9}{\partial M_S \partial H_U} \right]$$

But $v_8 = 0$(since M_S Component of eigenvector is 0), so the second term vanishes.
Thus:

$$a = 2w_2 v_1 v_9 \frac{\beta_1^*}{H_N}$$

Since $w_2 = 1$, $v_9 = 1$, $v_1 = \frac{\beta_1^* H_S^0}{H_N K_6} > 0$, we get:

$$a = \frac{2\beta_1^{*2} H_S^0}{H_N^2 K_6} > 0$$

According to Castillo-Chavez & Song [32] theorem $a > 0$ and $b > 0$ we have a backward bifurcation. This means:

1. For $R_0 < 1$, there exists an unstable endemic equilibrium alongside the stable DFE.
2. For $R_0 > 1$, there exists a stable endemic equilibrium and the DFE becomes unstable.

5 Optimal Control Analysis for the Dengue Model

This analysis aims to determine the most effective and cost-efficient strategy to reduce dengue prevalence by formulating and solving an optimal control problem. We will introduce time-dependent control measures into the model and define an objective functional to be minimized.

- u_1: Effort to reduce mosquito-human contact (e.g., using insect repellent, bed nets).
- u_2: Effort to test and identify infected individuals (symptomatic).
- u_3: Effort to treat confirmed infected individuals.
- u_4: Effort to control the mosquito population (e.g., insecticide spraying, larval source reduction).

The controlled system of differential equations becomes:

$$\left.\begin{aligned}
\tfrac{dH_S}{dt} &= \Lambda_1 - (1-u_1(t))\tfrac{\beta_1}{H_N} H_S M_I + \gamma_2 H_T + \xi_1 H_R - \mu_1 H_S,\\
\tfrac{dH_A}{dt} &= (1-u_1(t))\tfrac{\beta_1}{H_N} H_S M_I - (u_2(t)\alpha_1 + (1-u_2(t))\alpha_2 + \mu_1) H_A,\\
\tfrac{dH_T}{dt} &= u_2(t)\alpha_1 H_A - \gamma_1 H_T - \gamma_2 H_T \mu_1 H_T,\\
\tfrac{dH_U}{dt} &= (1-u_2(t))\alpha_2 H_A - \gamma_3 H_U - \mu_1 H_U,\\
\tfrac{dH_I}{dt} &= \gamma_1 H_T - u_3(t)\rho_1 H_I - \sigma_1 H_I - \mu_1 H_I,\\
\tfrac{dH_p}{dt} &= u_3(t)\rho_1 H_I + \gamma_3 H_U - \phi_1 H_p - \sigma_1 H_p,\\
\tfrac{dH_R}{dt} &= \phi_1 H_p - \xi_1 H_R - \mu_1 H_R,\\
\tfrac{dM_S}{dt} &= \Lambda_2 - (1-u_1(t))\tfrac{\beta_2}{H_N} M_S H_I - \tfrac{\beta_3}{H_N} M_S H_A - \tfrac{\beta_4}{H_N} M_S H_U - \tfrac{\beta_5}{H_N} M_S H_U - (\mu_2 + u_4(t)) M_S,\\
\tfrac{dM_I}{dt} &= (1-u_1(t))\tfrac{\beta_2}{H_N} M_S H_I + \tfrac{\beta_3}{H_N} M_S H_A + \tfrac{\beta_4}{H_N} M_S H_T + \tfrac{\beta_5}{H_N} M_S H_U - (\mu_2 + u_4(t)) M_I,
\end{aligned}\right\} \quad (30)$$

where,

- u_1:Reduces the force of infection in both directions (human to mosquito and mosquito to human) by a factor of $(1-u_1(t))$
- u_2:Increases the proportion of symptomatic individuals (H_A) who get tested (H_T) and decreases those who do not (H_U)
- u_3:Increases the rate at which confirmed infected individuals (H_I) receive treatment (H_P)
- u_4:Increases the mortality rate of both susceptible and infected mosquitoes.

The controls are bounded: $0 \le u_i(t) \le u_i^{max} \le 1$ for $i = 1, 2, 3, 4$, where u_i^{max} represents the maximum feasible implementation level of each control.

Our goal is to minimize the total cost over a fixed time period $[0, T]$. The cost includes:

- The cost associated with the disease itself (number of symptomatic, untreated, and infected individuals).
- The cost of implementing the control measures.

We define the objective functional $J(u_1, u_2, u_3, u_4)$ as:

$$J = \int_0^T \left[A_1 H_A(t) + A_2 H_I(t) + A_3 H_(H_U(t) + A_4 M_I(t) + \frac{1}{2}\sum_{i=1}^{4} B_i u_i^2(t) \right] dt$$

where A_1, A_2, A_3, A_4 : Weighting constants that balance the importance of reducing:

- A_1 Symptomatic but untested individuals (H_A).
- A_2 Confirmed infected individuals (H_I).
- A_3 Untested and unconfirmed individuals (H_U)
- A_4 Infected mosquitoes (M_I)

B_1, B_2, B_3, B_4 : Weighting constants representing the relative cost of implementing each control. Higher B_i implies a more expensive control.
The quadratic form $\frac{1}{2} B_i u_i^2(t)$ is standard in optimal control theory to model the nonlinear, increasing costs of control implementation (e.g., diminishing returns and societal resistance at high effort levels).

Our aim is to find optimal controls u_1^*,u_2^*, u_3^*, u_4^* such that:

$$J = (u_1^*, u_2^*, u_3^*, u_4^*) = \min_{u \in \mathcal{U}} J(u_1, u_2, u_3, u_4)$$

where $\mathcal{U}$ is the set of admissible (measurable and bounded) controls.

To find the optimal controls, we apply Pontryagin's Maximum Principle. This converts the problem into minimizing the Hamiltonian H point-wise with respect to the controls. **The Hamiltonian:**

$$\begin{aligned} H = [A_1 H_A(t) + A_2 H_I(t) + A_3 H_U(t) + A_4 M_I(t) + \frac{1}{2}(B_1 u_1^2(t) + B_2 u_2^2(t) + B_3 u_3^2(t) + B_4 u_4^2)] \\ + \lambda_S \frac{dH_S}{dt} + \lambda_A \frac{dH_A}{dt} + \lambda_T \frac{dH_T}{dt} + \lambda_T^- \frac{dH_U}{dt} \\ + \lambda_I \frac{dH_I}{dt} + \lambda_P \frac{dH_P}{dt} + \lambda_R \frac{dH_R}{dt} + \lambda_{S_m} \frac{dM_S}{dt} + \lambda_{I_m} \frac{dM_I}{dt} \end{aligned}$$

Where λ_S, λ_A, λ_T, λ_T^- ,λ_I, λ_P, λ_R,λ_{S_m}, λ_{I_m} are the adjoint variables (or costate variables) associated with each state variable.

The adjoint variables satisfy the following system of differential equations, derived from $\frac{d\lambda}{dt} = -\frac{\partial H}{\partial state}$:

$$\begin{aligned} \frac{d\lambda_S}{dt} &= -\frac{\partial H}{\partial H_S}, \frac{d\lambda_T}{dt} = -\frac{\partial H}{\partial H_T}, \frac{d\lambda_I}{dt} = -\frac{\partial H}{\partial H_I} \\ \frac{d\lambda_R}{dt} &= -\frac{\partial H}{\partial H_R}, \frac{d\lambda I_m}{dt} = -\frac{\partial H}{\partial M_I} \frac{d\lambda_A}{dt} = -\frac{\partial H}{\partial H_A} \\ \frac{d\lambda_T^-}{dt} &= -\frac{\partial H}{\partial H_U}, \frac{d\lambda_P}{dt} = -\frac{\partial H}{\partial H_P}, \frac{d\lambda_{S_m}}{dt} = -\frac{\partial H}{\partial M_S} \end{aligned}$$

These equations are solved backwards in time with the transversality conditions (terminal conditions):
$\lambda_S(T) = \lambda_A(T) = \lambda_T(T) = \lambda_T^-(T) = \lambda_I(T) = \lambda_P(T) = \lambda_R(T) = \lambda_(S_m)(T) = \lambda_(I_m)(T) = 0$

The optimal controls u_i^* are found by minimizing the Hamiltonian with respect to each u_i on the set $0 \leq u_i \leq u_i^{max}$. This is done by solving $\frac{\partial H}{\partial u_i} = 0$ subject to the bounds.

For u_1 (Prevention) :

$$\frac{\partial H}{\partial u_1} = B_1 u_1 + \frac{\beta_1}{H_N} H_S M_I (\lambda_S - \lambda_A) + \frac{\beta_2 H_I + \beta_3 H_A + \beta_4 H_T + \beta_5 H_U}{H_N} M_S (\lambda_{S_m} - \lambda_{I_m}) = 0$$

$$\implies u_1^* = \frac{\frac{\beta_1}{H_N} H_S M_I (\lambda_A - \lambda_S) + \frac{\beta_2 H_I + \beta_3 H_A + \beta_4 H_T + \beta_5 H_U}{H_N} M_S (\lambda_{I_m} - \lambda_{S_m})}{B_1}$$

$$u_1^* = max\left(0, min\left(u_1^{max}, \frac{\frac{\beta_1}{H_N} H_S M_I (\lambda_A - \lambda_S) + \frac{\beta_2 H_I + \beta_3 H_A + \beta_4 H_T + \beta_5 H_U}{H_N} M_S (\lambda_{I_m} - \lambda_{S_m})}{B_1}\right)\right)$$

For u_2 (Testing):

$$\frac{\partial H}{\partial u_2} = B_2 u_2 + \alpha_1 H_A (\lambda_A - \lambda_T) + \alpha_2 H_A (\lambda_T^- - \lambda_A) = 0$$

$$\implies u_2^* = \frac{\alpha_1 H_A (\lambda_T - \lambda_A) + \alpha_2 H_A (\lambda_A - \lambda_T^-)}{B_2}$$

$$u_2^* = max\left(0, min\left(u_2^{max}, \frac{\alpha_1 H_A (\lambda_T - \lambda_A) + \alpha_2 H_A (\lambda_A - \lambda_T^-)}{B_2}\right)\right)$$

For u_3 (Treatment):

$$\frac{\partial H}{\partial u_3} = B_3 u_3 + \frac{\rho_1 H_1 (\lambda_P - \lambda_I)}{B_3} = 0$$

$$\implies u_3^* = \frac{\alpha_1 H_A(\lambda_T - \lambda_A) + \alpha_2 H_A(\lambda_A - \lambda_T^-)}{B_2}$$

$$u_3^* = max\left(0, min\left(u_3^{max}, \frac{\rho_1 H_1(\lambda_P - \lambda_I)}{B_3}\right)\right)$$

For u_4 (Vector Control):

$$\frac{\partial H}{\partial u_4} = B_4 u_4 + M_S \lambda_{S_m} + M_I \lambda_{I_m} = 0$$

$$\implies u_4^* = \frac{M_S \lambda_{S_m} + M_I \lambda_{I_m}}{B_4}$$

$$u_4^* = max\left(0, min\left(u_4^{max}, \frac{M_S \lambda_{S_m} + M_I \lambda_{I_m}}{B_4}\right)\right)$$

6 Results

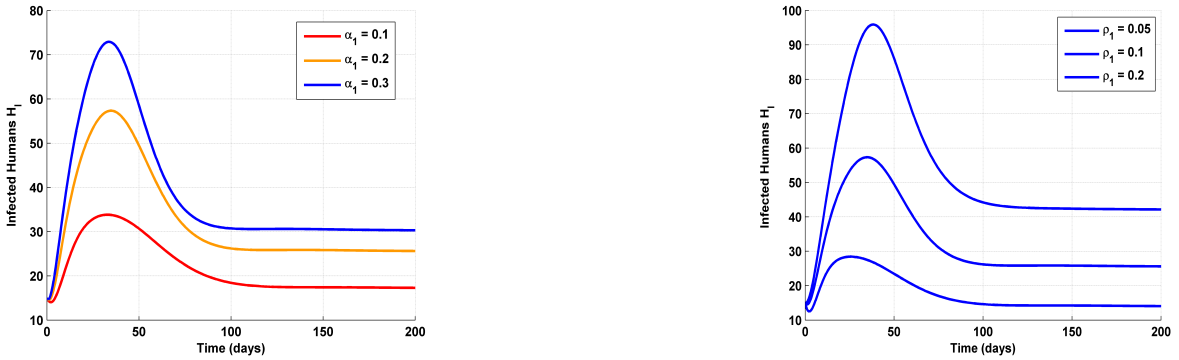

(a) (b)

Figure 2: Effect of Testing on Infected class (a) and Effect of Treatment on Infected Class (b)

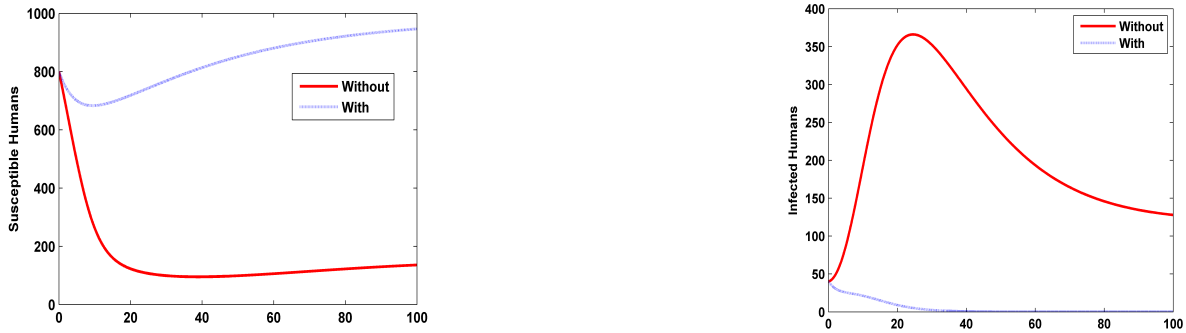

(a) (b)

Figure 3: Control Effect of Susceptible class (a) and Infected Human class (b)

The present section deals with numerical simulation of testing and treatment on infected class H_I and further it focuses on simulation of optimal control problem given in (Equation no. 24). Also, this section deals with the key findings of the study, supported by figures, tables, and statistical analysis. The proposed human–mosquito transmission model was numerically solved using efficient forward backward

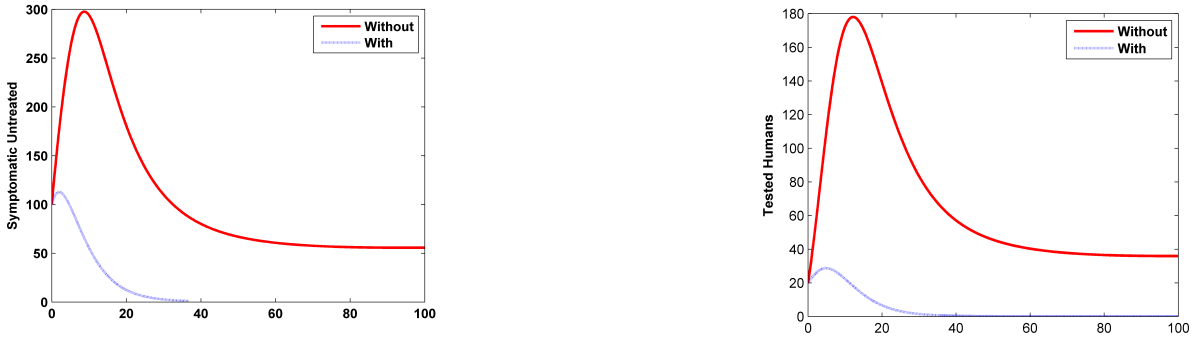

(a) (b)

Figure 4: Control Effect of symptomatic and untreated class (a) and tested class (b)

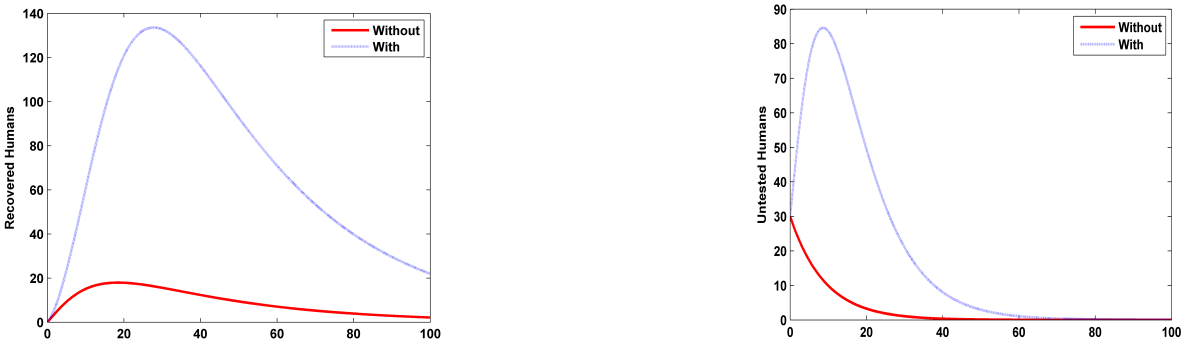

(a) (b)

Figure 5: Control Effect of recovered class (a) and Untested class (b)

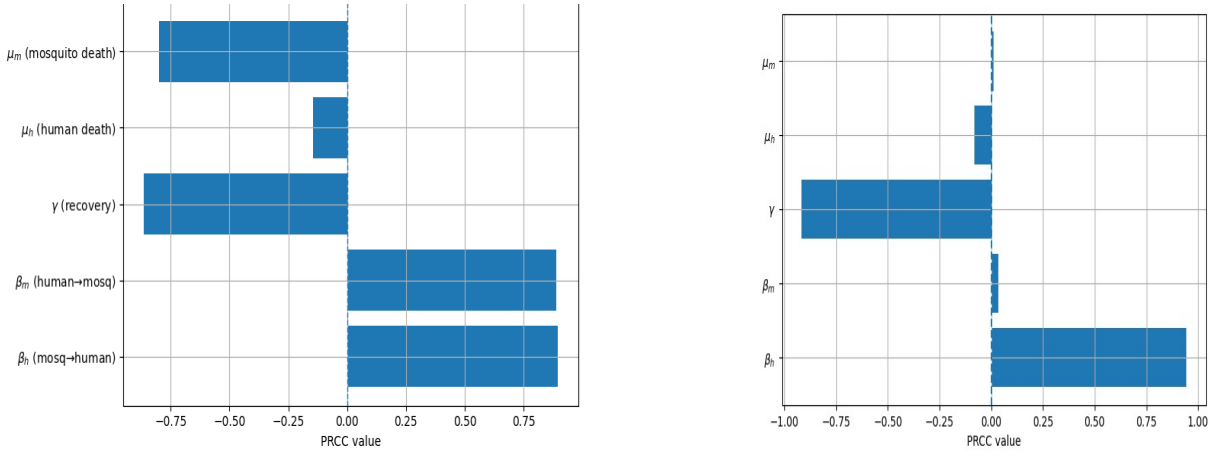

(a) (b)

Figure 6: PRCC of the basic reproduction number R_0 of model and PRCC of Peak Infection with respect to some model parameters shown in table 3 and 4.

sweep numerical scheme with the fourth-order Runge–Kutta optimization techniques with control strategies. Numerical simulations were carried out under two scenarios: without control interventions and with optimal control strategies applied to reduce disease transmission and progression of dengue fever pathogen among masses. The state variables considered include susceptible humans (H_S), symptotic human (H_A), tested human (H_T), human with no testing facility (H_U, infected human (H_I), hospitalized human (H_P), recovered (H_R), susceptible vector (M_S) and infected vector (M_I). Further, global sensitivity analysis technique is also used to check the influence of the parameters.

The Fig. 2 (a) presents effect of testing parameter on the number of detected and isolated infected humans under three different values of the parameter $\alpha_1 = 0.1, 0.2, 0.3$. It shows that there is an initial rapid detection of infected individuals, followed by a peak, and finally a decline towards a steady state. It means, as α_1 increases, the system detects a significantly higher volume of infections. For $\alpha_1 = 0.1$, it shows a low number of detected infected individuals which means, testing centers may unavailable or inaccessible. And hence, the majority of infected people remain untested and undetected and they spread the disease. For $\alpha_1 = 0.2$, the number of detected infected individuals rises significantly. This does not necessarily mean there are more sick people overall; rather, it means the health system is successful to identify them. It suggest that if we increase the testing resources then we can locate infected individuals who would otherwise be hidden in the population. For $\alpha_1 = 0.3$, it shows that higher testing allows us to identify and isolate a larger volume of people. When we detect a case, we can isolate that patient immediately. This prevents them from being bitten by mosquitoes and passing the virus to healthy people. Therefore, testing actually represents a more effective control strategy. For countries like Bangladesh and India, investing in testing availability is not just about counting cases but, it is one of the most effective tool to stop transmission.

Figure 2 (b) presents the impact of the treatment parameter, ρ_1 on the population of infected human. It shows that as the treatment parameter ρ_1 increases, both the peak number of infections and the steady-state burden of the disease decrease substantially. For $\rho_1 = 0.05$, we have limited treatment availability, the virus spreads widespread and infection also rises. This puts immense pressure on the healthcare system and increases the risk of severe complications and death. For $\rho_1 = 0.2$, we have better treatment facilities and we can drastically reduce the number of people suffering from the disease at any given time. It suggests that testing helps us to find the dengue infected individuals, treatment shows the profound impact that medical treatment has on the course of a dengue outbreak. In biological point of view, this represents people receiving medical care, recovering, and developing immunity. When a person is in the treatment class, they are no longer actively circulating the virus in the community. Results show that as we increase treatment options, the number of active infected people drops. This is because we are effectively shortening the time a person stays sick and infectious.
In Fig. 3 (a), the susceptible human population (H_S) exhibits a rapid decline in the absence of control, driven by sustained and intense exposure to a high density of infected mosquitoes. This quick decline reflects a high force of infection, characteristic of an environment with maximal vectorial capacity. Equally, upon the implementation of control measures, the interventions effectively lower the infection rate by reducing the effective contact rate and vector survival. Biologically, this indicates that preventive strategies disrupt the transmission cycle by creating a disconnect between vectors and hosts. If we limit the pathogen's ability to locate and infect susceptible individuals then these measures drive R0 below the critical threshold of unity, and hence significantly reduces the incidence of new infections and prevents an epidemic outbreak.

In Fig. 3 (b), the infected human population (H_I) exhibits a noticeable epidemic peak in the absence

of control, reflecting unrestricted community spread driven by a high basic reproduction number (R_0). The subsequent slow decline indicates that the pathogen continues to circulate strongly within the host population, persisting due to a high prevalence of infection and sustained vector density. However, under the control scenario, the peak magnitude of the infected population is substantially reduced. This shift signifies that interventions effectively break the chain of transmission, causing the outbreak to burn out rapidly rather than establishing a prolonged endemic state. Biologically, this indicates that reduced vectorial capacity and transmission probability are drastically lowering R_0, and decrease the disease burden and preventing the disease from reaching its full epidemic potential.

In Fig. 4 (a), the absence of intervention results in the prolonged persistence of symptotic (H_A) and human with no testing facility (H_U) individuals. This persistent incidence characterizes these cohorts as undiagnosed reservoirs. These individuals display clinical signs of dengue, yet by not utilizing or limiting availability of testing facilities, they avoid public health detection and subsequent isolation. Moreover, they remain integrated within the community, maintaining normal contact rates with domestic vectors and facilitating n continuous pathogen spillback. However, under the control regime, both populations decline significantly. This drastic reduction highlights the efficacy of active surveillance and satisfying intervention, which effectively identify and isolate infectious individuals, thereby reducing the duration of infectivity. Epidemiologically, this is vital for suppressing undetected transmission and it ensures that the pathogen cannot propagate from ill individuals to new vectors.

In Fig. 4 (b), the implementation of control measures triggers an initial surge in the tested human population (H_T) that suggest a direct impact of enhanced surveillance sensitivity and active case detection. This peak illustrates the system's success in capturing infectious individuals during their acute phase, effectively identifying the pathogen's presence before it can spread widely. Over time, the epidemiological burden on healthcare systems lessens significantly due to severe cases need hospitalization. This trend demonstrates that early diagnostic intervention fundamentally changes the natural history of the infection. It means, if we can support prompt clinical management such as fluid resuscitation and monitoring, early testing then it can effectively prevents the progression to severe pathophysiology. Therefore, this reduces the overall morbidity rate and prevents the saturation of critical care resources. Hence, the rapid detection and isolation are key to mitigating both transmission and clinical severity.

In Fig. 5 (a), the dynamics of the recovered population reveal a critical difference in disease outcomes. The 'with control' strategy demonstrates a higher accumulation of individuals in the recovered compartment, reflecting a high rate of successful clinical resolution and immunity acquisition. Conversely, in the absence of control, the recovered population significantly decreases; this reduction is biologically driven by elevated mortality rates and the exhaustion of the susceptible pool, which naturally curtails the flow of individuals moving from the infected to the recovered state. This behavioral contrast confirms that the synergistic effects of prevention, treatment, and vector management drastically reduce the overall disease burden.

In Fig.5 (b), the implementation of control measures triggers an initial decline in the untested human population (H_U) which suggests the direct transfer of individuals from the untested into the tested and monitored groups, due to enhanced surveillance sensitivity and active case detection. This downward trend illustrates the system's success in narrowing the pool of unidentified infections, effectively reducing the number of individuals who could unknowingly transmit the pathogen. Over time, the untested population stabilizes at a lower level, demonstrating that sustained detection efforts continuously limit the reservoir of hidden infection. This trend indicates that early and persistent diagnostic intervention funda-

mentally alters the transmission landscape. It means that if proactive testing campaigns and community screening are maintained, a smaller proportion of the population remains unclassified and potentially infectious. Therefore, this reduces the overall force of infection and prevents unchecked community spread. Hence, the rapid and continuous reallocation of individuals from the untested to the tested compartment is key to mitigating silent transmission and achieving epidemic control.

In short, our research proves that taking action saves lives. By combining mosquito control, early testing, and effective treatment, we can significantly stop the spread of disease. This approach keeps more people healthy, reduces the number of severe outbreaks, and is a smart investment for public health. Therefore, having a plan is far better than doing nothing, providing a clear road-map for protecting our communities from dangerous vector-borne diseases.

Partial Rank Correlation Coefficient (PRCC) analysis

Partial Rank Correlation Coefficient (PRCC) is a global sensitivity analysis technique used to determine how model outputs depend on uncertain input parameters while accounting for the influence of other parameters. A global sensitivity analysis was carried out using the Partial Rank Correlation Coefficient (PRCC) method combined with Latin Hypercube Sampling (LHS). The basic reproduction number R_0 was chosen as the response function. The PRCC results indicate that the transmission parameters β_h and β_m have strong positive correlations with R_0 while the recovery rate γ and mosquito mortality rate μ_m exhibit strong negative correlations. This suggests that reducing transmission and increasing recovery or vector mortality are effective strategies for disease control. Each parameter was varied over a biologically realistic range using Latin Hypercube Sampling (LHS) with 500 samples.

PRCC Analysis of R_0: The basic reproduction number R_0 was chosen as the response variable, as it determines disease invasion and persistence in the population. Key epidemiological parameters associated with human–mosquito transmission and disease progression were varied simultaneously over biologically realistic ranges using Latin Hypercube Sampling (LHS). This ensures uniform and efficient exploration of the multidimensional parameter space. For each sampled parameter set, the corresponding value of R_0 was computed using the analytical expression derived from the model. Both the input parameters and the model output were rank-transformed, and PRCC values were calculated to measure the monotonic relationship between each parameter and R_0, while controlling for the influence of all other parameters. The Fig.5 this measures the monotonic relationship between each input parameter and the model output R_0, while accounting for the effects of other parameters. The values range from -1 to 1:
Positive PRCC (β_h and β_m): A positive value indicates that as the parameter's rank increases, the R_0 rank also tends to increase. This suggests a direct relationship.
Negative PRCC (γ, μ_h and μ_m): A negative value indicates an inverse relationship; as the parameter's rank increases, the R_0 rank tends to decrease. The absolute value of PRCC reflects the strength of influence. It is also concluded from plot that the human–mosquito transmission rate and mosquito–human transmission rate exhibit strong positive PRCC values, indicating that these parameters significantly enhance disease spread. The human recovery rate and mosquito mortality rate show strong negative PRCC values, implying that increasing recovery or reducing mosquito lifespan effectively suppresses disease transmission. The parameters with PRCC values close to zero have relatively minor influence on R_0. In our results, all p-values are extremely small (close to 0), indicating that all the calculated PRCC values are statistically significant. This means you can be confident that the relationships observed between the parameters and R0 are real and not due to random variation. Thus, PRCC analysis not only supports the analytical results obtained from the basic reproduction number but also provides quantitative evidence for prioritizing control strategies in the dengue transmission framework.

Parameter uncertainty was explored using Latin Hypercube Sampling, and PRCC values were computed following rank transformation of inputs and outputs. The results indicate that transmission parameters exhibit strong positive and statistically significant correlations with peak infection ($\rho < 0.05$) demonstrating their dominant role in determining outbreak intensity. In contrast, recovery and removal-related parameters show significant negative PRCC values ($\rho < 0.05$)), indicating their effectiveness in reducing the maximum number of infected individuals. Parameters with PRCC values close to zero were not statistically significant and had minimal influence on the epidemic peak. Overall, the PRCC analysis confirms that epidemic peak severity is primarily driven by transmission dynamics, while enhanced recovery and removal mechanisms significantly mitigate outbreak intensity.

Table 2: PRCC and p-values of sensitive parameters

Parameter	**PRCC**	**p-values**
β_h	0.894784218784219	0.0
β_m	0.8901108261108263	0.0
γ	-0.862831750831751	$5.92075608457 \times 10^{-298}$
μ_h	-0.144745368745368	$4.3119952320674 \times 10^{-6}$
μ_m	-0.7993624873624874	$5.0950101498717 \times 10^{-223}$

Table 3: PRCC and p-values of model parameters for analysis of peak infection

Parameter	PRCC	p-values
β_h	0.9462093528374111	3.397844291919171e-246
β_m	-0.02020491281965128	0.6521979920871408
γ	-0.8951313885255541	7.480509672254369e-177
μ_h	-0.16994650378601514	0.00013430945590220695
μ_m	-0.031337501350005396	0.4844609689287612

7 Policy Implications of Integrating Testing and Treatment

The integration of testing and treatment pathways into the dengue transmission model reveals critical epidemiological shifts that are invisible in traditional models focusing solely on vector control. Our proposed model considering testing and treatment showed against a baseline scenario where these clinical pathways are absent. From this investigations, we can derive specific policy recommendations for Bangladesh, India, and similar endemic regions.

In standard dengue models (without explicit testing and treatment), the basic reproduction number, R_0 is primarily driven by vector parameters (mosquito density and biting rates). In our model, R_0 is explicitly controlled by clinical parameters. If we remove the intervention terms such as $\alpha_1 \to 0$, $\rho_1 \to 0$), the "drain" from the infectious compartments is reduced to natural recovery only. Mathematically, the denominators in the R_0 expression decrease and it shows R_0 to increase significantly. This implies that in a system without testing and treatment, the disease is intrinsically more robust and requires far more aggressive vector control to bring R_0 below the critical threshold of 1. The terms α_1 (testing rate) and ρ_1 (treatment rate) appear in the denominators of the transmission components. This confirms that these interventions act to reduce the effective R_0 by shortening the infectious period. Therefore, policies that invest in healthcare infrastructure act as a direct biological brake on the epidemic, independent of killing

mosquitoes.

Our analysis reveals the phenomenon of backward bifurcation, where a stable endemic equilibrium coexists with the disease-free equilibrium even when $R_0 < 1$. This suggest that even if interventions temporarily reduce R_0 below 1, the disease may persist unless effort is drastically increased. When we consider the models without testing and treatment, backward bifurcation is often driven solely by complex vector dynamics or imperfect vaccines. This makes policy "fragile," where reduction of mosquito counts slightly fails to stop the outbreak. However, if we include testing and treatment, it alters the flow of the system. If we can identify infectious individuals and moving them to the treated class, we reduce the effective force of infection. Thus, a policy that integrate testing is more likely to result in a clear "threshold effect" and helps to push the system deterministically toward elimination without requiring impossibly high levels of vector control.

The optimal control analysis compared four controls: prevention, testing, treatment, and vector control. If policy relies solely on insecticide and nets, the cost function rises rapidly. Insecticide resistance (a rising problem in Bangladesh and India) means transmission rates does not drop linearly with cost. The economic burden of continuous fogging is unsustainable. Our simulation results suggest that a moderate application of testing and treatment combined with vector control achieves lower prevalence at a lower total cost.

8 Discussion and Conclusion

This study presents a novel mathematical model for dengue transmission that integrates testing and treatment dynamics components often underrepresented in existing epidemiological frameworks. By explicitly modeling pathways from symptomatic infection through testing, confirmation, treatment, and recovery, the framework captures critical public health realities in dengue-endemic settings like Bangladesh and India. The analytical derivation of (R_0) and stability analyses confirm that the disease-free equilibrium is globally asymptotically stable when $(R_0 < 1)$, while an endemic equilibrium emerges and stabilizes when $(R_0 > 1)$. Notably, the model exhibits backward bifurcation, implying that dengue can persist even when $(R_0 < 1)$ under certain conditions, highlighting the challenge of elimination in the presence of asymptomatic carriers and inadequate testing.

Further bifurcation analyses reveal rich dynamical behavior:Hopf bifurcation leads to sustained periodic outbreaks, mimicking observed multi-year epidemic cycles; saddle-node bifurcation induces bistability and hysteresis, explaining why dengue is harder to eradicate once established; and Bogdanov–Takens bifurcation acts as an organizing center for transitions between disease-free, endemic, and oscillatory states. These nonlinear phenomena underscore the complexity of dengue dynamics and the limitations of conventional threshold-based control policies.

The optimal control analysis identifies synergistic intervention strategies, emphasizing that combined efforts in personal protection (u_1), enhanced testing (u_2), timely treatment (u_3), and vector control (u_4) are more effective and cost-efficient than isolated measures. Specifically, improving diagnostic coverage and treatment access not only reduces morbidity and mortality but also dampens oscillatory transmission patterns, leading to more predictable and manageable outbreaks. Also, the PRCC results identify transmission and vector-related parameters as the most influential factors governing dengue dynamics, highlighting vector control and improved treatment as the most effective intervention strategies.

In summary, this research provides a robust, integrative modeling tool that bridges gaps between theoretical epidemiology and public health practice. The findings offer actionable insights for policymakers in dengue-endemic regions, supporting the design of resilient, adaptive, and evidence-based control programs tailored to local epidemiological and infrastructural contexts. Future work should focus on parameter estimation using real-world data and the incorporation of spatial heterogeneity, climate variables,

and socio-behavioral factors to further enhance model predictive power and policy relevance.

Several mathematical extensions could enhance the theoretical depth and analytical richness of the proposed framework. The model could be extended to incorporate multi-strain dynamics with cross-immunity structures, allowing the study of serotype competition and antibody-dependent enhancement through a coupled system of differential equations. Introducing spatial diffusion via reaction-diffusion or meta-population formulations would enable analysis of traveling wave solutions and pattern formation in heterogeneous environments. The current deterministic framework could be extended to include stochastic elements through Itô or Stratonovich calculus to study extinction probabilities and noise-induced transitions between equilibria. Incorporating age-structure using McKendrick-von Foerster partial differential equations would allow analysis of age-dependent transmission and immunity profiles. Finally, developing a fractional-order derivative version of the model could capture memory effects and non-local transmission dynamics, offering new perspectives on dengue's temporal evolution.

References

[1] Islam, M. S., Shahrear, P., Saha, G., Ataullha, M., & Rahman, M. S. (2024). Mathematical analysis and prediction of future outbreak of dengue on time-varying contact rate using machine learning approach. *Computers in Biology and Medicine*, 178, 108707. doi:10.1016/j.compbiomed.2024.108707

[2] Ghosh, I., Tiwari, P. K., & Chattopadhyay, J. (2019). Effect of active case finding on dengue control: Implications from a mathematical model. *Journal of Theoretical Biology*, 464, 50–62. doi:10.1016/j.jtbi.2018.12.027

[3] Aldila, D., Ndii, M. Z., Anggriani, N., Windarto, Tasman, H., & Handari, B. D. (2023). Impact of social awareness, case detection, and hospital capacity on dengue eradication in Jakarta: A mathematical model approach. *Alexandria Engineering Journal*, 64, 691–707. doi:10.1016/j.aej.2022.11.032

[4] Sharma, N., Singh, R., Cattani, C., & Pathak, R. (2021). Modeling and complexity in dynamics of T-cells and cytokines in dengue fever based on antiviral treatment. *Chaos, Solitons and Fractals*, 153, 111448. doi:10.1016/j.chaos.2021.111448

[5] Naaly, B. Z., Marijani, T., Isdory, A., & Ndendya, J. Z. (2024). Mathematical modeling of the effects of vector control, treatment and mass awareness on the transmission dynamics of dengue fever. *Computer Methods and Programs in Biomedicine Update*, 6, 100159. doi:10.1016/j.cmpbup.2024.100159

[6] Venkatesh, A., Prakash Raj, M., & Baranidharan, B. (2024). Analyzing dynamics and stability of single delay differential equations for the dengue epidemic model. *Results in Control and Optimization*, 15, 100415. doi:10.1016/j.rico.2024.100415

[7] Din, A., Khan, T., Li, Y., Tahir, H., Khan, A., & Khan, W. A. (2021). Mathematical analysis of dengue stochastic epidemic model. *Results in Physics*, 20, 103719. doi:10.1016/j.rinp.2020.103719

[8] Puspita, J. W., Farida, Fakhruddin, M., Nuraini, N., Fauzi, R., Indratno, S. W., & Soewono, E. (2023). Modeling and descriptive analysis of dengue cases in Palu City, Indonesia. *Physica A*, 625, 129019. doi:10.1016/j.physa.2023.129019

[9] Saha, P., Sikdar, G. C., Ghosh, J. K., & Ghosh, U. (2023). Disease dynamics and optimal control strategies of a two serotypes dengue model with co-infection. *Mathematics and Computers in Simulation*, 209, 16–43. doi:10.1016/j.matcom.2023.02.011

[10] Ren, H., & Xu, R. (2025). Transmission dynamics of dengue with asymptomatic infection and a case study in Bangladesh. *Mathematics and Computers in Simulation*, 231, 1–18. doi:10.1016/j.matcom.2024.12.003

[11] Wang, Y., Zhao, S., Wei, Y., Li, K., Jiang, X., Li, C., Ren, C., Yin, S., Ho, J., Ran, J., Han, L., Zee, B. C., & Chong, K. C. (2023). Impact of climate change on dengue fever epidemics in South and Southeast Asian settings: A modelling study. *Infectious Disease Modelling*, 8(3), 645–655. doi:10.1016/j.idm.2023.05.008

[12] Guo, S., He, M., & Li, F. (2025). Threshold dynamics of a time-delayed dengue virus infection model incorporating vaccination failure and exposed mosquitoes. *Applied Mathematics Letters*, 161, 109366. doi:10.1016/j.aml.2024.109366

[13] El-shenawy, A., El-Gamel, M., & Teba, A. (2024). Simulation of the SIR dengue fever nonlinear model: A numerical approach. *Partial Differential Equations in Applied Mathematics: A Spin-off of Applied Mathematics Letters*, 11, 100891. doi:10.1016/j.padiff.2024.100891

[14] de Araujo, A. L. A., Boldrini, J. L., Calsavara, B. M. R., & Correa, M. R. (2025). Analysis and numerical approximation of a mathematical model for Aedes aegypti populations. *Computers & Mathematics with Applications*, 180, 214–241. doi:10.1016/j.camwa.2025.01.014

[15] Fauzi, I. S., Nuraini, N., Ayu, R. W. S., Wardani, I. B., & Rosady, S. D. N. (2025). Seasonal pattern of dengue infection in Singapore: A mechanism-based modeling and prediction. *Ecological Modelling*, 501, 111003. doi:10.1016/j.ecolmodel.2024.111003

[16] Zhang, J., Liu, L., Li, Y., & Wang, Y. (2023). An optimal control problem for dengue transmission model with Wolbachia and vaccination. *Communications in Nonlinear Science & Numerical Simulation*, 116, 106856. doi:10.1016/j.cnsns.2022.106856

[17] Li, Y., Wang, Y., & Liu, L. (2023). Optimal control of dengue vector based on a reaction–diffusion model. *Mathematics and Computers in Simulation*, 203, 250–270. doi:10.1016/j.matcom.2022.06.026

[18] Ten Bosch, Q. A., Clapham, H. E., Lambrechts, L., Duong, V., Buchy, P., Althouse, B. M., ... & Salje, H. (2020). Contributions from the silent majority dominate dengue virus transmission. *PLOS Pathogens*, 16(5), e1008415.

[19] Silva, S. J. R. D., Pena, L., & Magalhães, J. J. (2021). Modeling the transmission dynamics of dengue fever: implications of temperature effects, vector control, and transovarial transmission. *Journal of Theoretical Biology*, 524, 110731.

[20] Chan, M., & Johansson, M. A. (2019). The incubation periods of dengue viruses: A systematic review and meta-analysis. *Epidemiology & Infection*, 147, e200.

[21] Kramer, L. D., & Ciota, A. T. (2019). Dissecting vectorial capacity for mosquito-borne viruses. *Current Opinion in Virology*, 35, 48-55.

[22] Wilder-Smith, A., Ooi, E. E., Horstick, O., & Wills, B. (2019). Dengue. *The Lancet*, 393(10169), 350-363.

[23] Reich, N. G., Shrestha, S., King, A. A., Rohani, P., Lessler, J., Kalayanarooj, S., ... & Cummings, D. A. (2013). Interactions between serotypes of dengue highlight epidemiological impact of cross-immunity. *Journal of The Royal Society Interface*, 10(86), 20130414.

[24] Katzelnick, L. C., Ben-Shachar, R., Mercado, J. C., Rodriguez-Barraquer, I., Elizondo, D., Arguello, S., ... & Harris, E. (2020). Dynamics and determinants of the force of infection of dengue virus from 1994 to 2015 in Managua, Nicaragua. *Proceedings of the National Academy of Sciences*, 117(52), 33821-33827.

[25] Van den Driessche, P. and Watmough, J. Reproduction numbers and sub-threshold endemic equilibria for compartmental models of disease transmission. *Mathematical Biosciences*, 180(1-2):29–48, 2002. doi: 10.1016/S0025-5564(02)00108-6.

[26] Kuznetsov, Y. A. (1998). *Elements of Applied Bifurcation Theory* (2nd ed.). Springer-Verlag, New York.

[27] Guckenheimer, J., & Holmes, P. (1983). *Nonlinear Oscillations, Dynamical Systems, and Bifurcations of Vector Fields*. Springer-Verlag, New York.

[28] Martcheva, M. (2015). *An Introduction to Mathematical Epidemiology*. Springer, New York.

[29] Bogdanov, R. I. (1981). Bifurcations of a limit cycle for a family of vector fields on the plane. *Selecta Mathematica Sovietica*, 1(4), 373-388.

[30] Verma, V. S., Kaushik, H., Singh, R., Jain, S., & Akgül, A. (2024). Stability and Hopf bifurcation of TB-COVID-19 coinfection model with impact of time delay. SeMA Journal, 1-41.

[31] Takens, F. (1974). Singularities of vector fields. *Publications Mathématiques de l'IHÉS*, 43, 47-100.

[32] Castillo-Chavez, C., & Song, B. (2004). Dynamical models of tuberculosis and their applications.*Mathematical Biosciences & Engineering*, 1(2), 361–404.

Appendix A: Coefficients of the Characteristic Polynomial

This appendix provides the mathematical framework for obtaining the coefficients C_i $(i = 0, 1, \ldots, 8)$ of the characteristic polynomial associated with the Jacobian matrix evaluated at the endemic equilibrium X^* of the dengue transmission model (Section 5.2). The characteristic equation is:

$$\lambda^9 + C_8\lambda^8 + C_7\lambda^7 + C_6\lambda^6 + C_5\lambda^5 + C_4\lambda^4 + C_3\lambda^3 + C_2\lambda^2 + C_1\lambda + C_0 = 0.$$

Compressed Matrix Notation

Given the Jacobian matrix $J(X^*)$, let $M^{(k)}$ denote the sum of all its $k \times k$ principal minors. The coefficients C_i of the characteristic polynomial $P(\lambda) = \det(J - \lambda I)$ are given by the Faddeev-LeVerrier recursive relations are explained below :
The Faddeev-LeVerrier algorithm computes the coefficients C_i of the characteristic polynomial

$$P(\lambda) = \det(J - \lambda I) = (-\lambda)^n + C_1(-\lambda)^{n-1} + C_2(-\lambda)^{n-2} + \cdots + C_n$$

recursively as follows:

$$
\begin{aligned}
M^{(1)} &= \operatorname{tr}(J), & C_1 &= -M^{(1)} \\
M^{(2)} &= \frac{1}{2}\operatorname{tr}\left(J^2 + C_1 J\right), & C_2 &= -\frac{1}{2}M^{(2)} \\
&\vdots & &\vdots \\
M^{(k)} &= \frac{1}{k}\operatorname{tr}\left(J^k + C_1 J^{k-1} + \cdots + C_{k-1} J\right), & C_k &= -\frac{1}{k}M^{(k)}
\end{aligned}
$$

where $M^{(k)}$ denotes the sum of all $k \times k$ principal minors of J.
Similalry applying this to our characterstic polynomial we get,

$$
\begin{aligned}
C_8 &= -\operatorname{tr}(J) = -M^{(1)}, \\
C_7 &= -\frac{1}{2}\left(C_8 \operatorname{tr}(J) + \operatorname{tr}(J^2)\right) = M^{(2)}, \\
C_6 &= -\frac{1}{3}\left(C_7 \operatorname{tr}(J) + C_8 \operatorname{tr}(J^2) + \operatorname{tr}(J^3)\right) = -M^{(3)}, \\
&\vdots \\
C_0 &= \frac{1}{9}\left(C_1 \operatorname{tr}(J) + C_2 \operatorname{tr}(J^2) + \cdots + C_8 \operatorname{tr}(J^8) + \operatorname{tr}(J^9)\right) = \det(J).
\end{aligned}
$$

To implement these formulas explicitly, the Jacobian at the endemic equilibrium is structured as:

$$
J(X^*) = \begin{bmatrix} J_{HH} & J_{HV} \\ J_{VH} & J_{VV} \end{bmatrix},
$$

where the blocks correspond to human (H) and vector (V) compartments. The non-zero blocks are:

$$
J_{HH} = \begin{bmatrix} -(\mu_h + \zeta_1 I_v^*) & 0 & 0 & -\zeta_1 S_h^* \\ \zeta_1 I_v^* & -(\mu_h + \gamma_h) & 0 & \zeta_1 S_h^* \\ 0 & \gamma_h & -(\mu_h + \delta_h) & 0 \\ 0 & 0 & \delta_h & -\mu_h \end{bmatrix},
$$

$$
J_{HV} = \begin{bmatrix} 0 & -\beta_{hv} S_h^*/N_h^* & 0 \\ 0 & \beta_{hv} S_h^*/N_h^* & 0 \\ 0 & 0 & 0 \\ 0 & 0 & 0 \end{bmatrix},
$$

$$
J_{VH} = \begin{bmatrix} 0 & 0 & 0 & 0 \\ -\beta_{vh} I_v^*/N_h^* & \beta_{vh} S_v^*/N_h^* & 0 & 0 \\ 0 & 0 & 0 & 0 \end{bmatrix}^\top,
$$

$$
J_{VV} = \begin{bmatrix} -(\mu_v + \zeta_2 I_h^*) & 0 & 0 \\ \zeta_2 I_h^* & -(\mu_v + \gamma_v) & 0 \\ 0 & \gamma_v & -\mu_v \end{bmatrix}.
$$

Here, $\zeta_1 = \beta_{hv}/N_h^*$, $\zeta_2 = \beta_{vh}/N_h^*$. The coefficients C_i are polynomials in the entries of these matrices. For brevity, we provide the three most structurally significant coefficients:

$C_8 = (2\mu_h + \gamma_h + \delta_h) + (2\mu_v + \gamma_v) + (\zeta_1 I_v^* + \zeta_2 I_h^*)$,

$C_4 =$ (Positive sum of products of 5 diagonal entries, adjusted for off-diagonal transmission terms)

$C_0 = \mu_h^2 \mu_v (\mu_h + \gamma_h)(\mu_h + \delta_h)(\mu_v + \gamma_v) \times$
$\big[(\mu_h + \zeta_1 I_v^*)(\mu_v + \zeta_2 I_h^*) - (\zeta_1 S_h^*)(\zeta_2 S_v^*)\big]$.

The full set of C_i can be generated algorithmically from the matrix J above using the recursive formulas.

Tabular Form with Key Components

Coefficient	Algebraic Form
C_8	$-(a_1 + a_2 + a_3 + 3a_4 + b_1 + b_2 + 2b_3)$
C_7	$a_1a_2 + a_1a_3 + a_1a_4 + a_2a_3 + a_2a_4 + a_3a_4 + a_4^2 + b_1b_2 + b_1b_3 + b_2b_3$ $+b_3^2 + (a_1 + a_2 + a_3 + 3a_4)(b_1 + b_2 + 2b_3) - \zeta_1\zeta_2$
C_6	$-\big[(a_1a_2a_3 + a_1a_2a_4 + a_1a_3a_4 + a_2a_3a_4) +$ (similar 3-term human combos) $+$(vector combos) + (cross-terms) $+ (\zeta_1\zeta_2)(a_1 + a_2 + b_1 + b_2)\big]$
C_5	Sum of 120 four-factor products from diagonal, minus corrections from off-diagonals
C_4	$-$Sum of 126 five-factor principal minors
C_3	Sum of 84 six-factor principal minors
C_2	$-$Sum of 36 seven-factor principal minors
C_1	Sum of 9 eight-factor principal minors
C_0	$\det(J) = \prod_{i=1}^{4} \alpha_i \cdot \prod_{j=1}^{3} \beta_j - \zeta_1\zeta_2 S_h^* S_v^* \cdot (\alpha_3\alpha_4\beta_3)$

where:

$$\alpha_1 = \mu_h + \zeta_1 I_v^*, \quad \alpha_2 = \mu_h + \gamma_h, \quad \alpha_3 = \mu_h + \delta_h, \quad \alpha_4 = \mu_h,$$
$$\beta_1 = \mu_v + \zeta_2 I_h^*, \quad \beta_2 = \mu_v + \gamma_v, \quad \beta_3 = \mu_v.$$

where:

$$\alpha_1 = \mu_h + \zeta_1 I_v^*, \quad \alpha_2 = \mu_h + \gamma_h, \quad \alpha_3 = \mu_h + \delta_h, \quad \alpha_4 = \mu_h,$$
$$\beta_1 = \mu_v + \zeta_2 I_h^*, \quad \beta_2 = \mu_v + \gamma_v, \quad \beta_3 = \mu_v.$$

Declarations

Availability of data and materials: No data is used in this study. Data are generated using mathematical model.

Acknowledgment This research work is supported by the Jammu and Kashmir Science Technology and Innovation Council(JKST&IC) No: JKST&IC/J/14/2022/409-13, Department of Science and Technology, Government of Jammu and Kashmir.

Conflicts of interest: All authors declared that there is no conflicts of interest to disclose.

Ethical approval and consent to participate: Not applicable.

Use of Artificial Intelligence Tools: Generative artificial intelligence (AI) tools, specifically ChatGPT (GPT-3.5 model), were used in this study to assist with language refinement, grammar checking, and improving the clarity and flow of the Introduction section.